Waves in Random and Complex Media
Vol. 00, No. 00, July 2011, 1–25

ARTICLE

Analysis of the Multiple Reflections by Strong Interfaces in Random Media

Maarten V. de Hoop[a], Josselin Garnier[b] and Knut Solna[c*]

[a] *Center for Computational and Applied Mathematics, Purdue University, 150 N. University Street, West Lafayette IN 47907, USA*; [b] *Laboratoire de Probabilités et Modèles Aléatoires & Laboratoire Jacques-Louis Lions, Université Paris 7, Site Chevaleret, 75205 Paris Cedex 13, France*; [c] *Department of Mathematics, University of California at Irvine, Irvine, CA 92697-3875, USA*

(*July 2011*)

We study scalar waves probing an heterogeneous medium whose parameters are modeled in terms of a statistically isotropic random process. The medium is terminated by an oblique interface and pressure release type boundary conditions at the other end. The tilt of the interface is relatively small so that the main wave field is confined to a paraxial tube. This formulation generalizes the classic situation of the Itô-Schrödinger equations since the medium macroscale features are not purely one dimensional. It provides the first step toward analysis of the situation with propagation in general three-dimensional background media modulated by random microstructure.
The situation with heterogeneous interface of phase transition zones with a tilt is important to model characteristic situations in reflection seismology. We have started the study of this case generalizing the invariant imbedding techniques used in the case of homogeneous interfaces and one-dimensional macroscale features.
We discuss in detail the enhanced backscattering phenomenon or weak localization in this setting with a tilted interface imbedded in the medium and find that the backscattering cone does not depend on the tilt.

Keywords: Paraxial approximation, enhanced backscattering, random media, oblique interface, free surface boundary condition

1. Introduction

We consider scalar waves propagating in a heterogeneous medium. We model the heterogeneities as a a realization of a random field with relatively short scale medium fluctuations. We want to characterize the waves that have been reflected from the random medium. The configuration we consider here corresponds to beam or long range propagation. Such a situation is often modeled by paraxial wave equations. In the last decades the paraxial wave equation has emerged as the dominant tool to describe small scale scattering situations such as in radiowave propagation, radar, remote sensing, propagation in urban environments and in underwater acoustics, moreover, for propagation problems in the earth's crust, [1, 3]. In the classic situation this approximation leads to only forward propagating waves, a forward-scattering approximation. Here we consider a generalization that captures also the reflected wave. Such a generalization is important for instance from the point of view of applications to imaging. In [6] we considered the situation with a

*Corresponding author. Email: ksolna@math.uci.edu

ISSN: 0278-1077 print/ISSN 1745-5049 online

DOI: 10.1080/1745503YYxxxxxxxx
http://www.informaworld.com

horizontal interface. There we showed that both the paraxial approximation associated with the beam geometry and a white noise approximation associated with the rapid medium fluctuations can be justified simultaneously. For the transmitted field the limit equation should take the form of the random Schrödinger equation studied in particular in [4].

In this paper we generalize this to the situation with a tilted interface at the bottom of the random slab, generating strong reflection, moreover, the situation with a pressure release, or free surface, boundary condition at the top interface of the random slab that we consider. Such a generalization is relevant in for instance reflection seismology and the paper can be seen as a first step toward understanding situations with a general background variation. This situation that we now consider generates multiple reflections and we derive a characterization of these, in distribution, in terms of a family of reflection operators whose kernels satisfy Itô-Schrödinger equations. We discuss in detail how these lead to specific problems for Wigner transforms of the limit kernels that are useful for analyzing the characteristics of the reflected wave field. We use this representation to analyze the spreading and decorrelation of the reflected field. As a specific application of our result we also consider the enhanced backscattering phenomenon or weak localization effect [2, 9]: if a quasi-plane wave is incoming with a given incidence angle, then the mean reflected intensity has a local maximum in the backscattered direction, which is twice as large as the mean reflected intensity in the other directions. This enhancement can be observed in a small cone around the backscattered direction, and it can be interpreted as the result of constructive interferences between reciprocal wave paths. The result we find here is very interesting in that in our configuration the backscattering cone depends on the presence of the bottom interface, but does not depend on the tilt. This emphasizes the fact that the enhanced backscattering phenomenon is a coherence effect. We remark that in this paper we analyze the partially coherent wave energy being reflected from the interface and the free surface. The situation is different if one consider the wave energy that is reflected by the random fluctuations only, such a situation is discussed in [5].

The outline of the paper is as follows. We introduce the model and the main separation of scales assumption in Section 2. In Section 3 we carry out the basic wave decomposition in locally up- and down-propagating wave components. This leads to a boundary value formulation and we convert this to an initial value formulation via invariant imbedding in Section 4. We present the main result in Section 5 that shows how we can characterize the wave reflection process and the multiples associated with our formulation via an Itô-Schrödinger equation for the reflection operator. After a brief review of the form of the reflected field in the homogeneous case presented in Section 6, we discuss in detail in Section 7 how the microstructure in our configuration affects the first and second (cross) moments of the reflected field. We finish with a discussion of the enhanced backscattering phenomenon in Section 8.

2. Scaling and Assumptions

We consider acoustic waves propagating in $1 + d$ spatial dimensions with random medium fluctuations. The governing equations are

$$\rho(z,\boldsymbol{x})\frac{\partial \boldsymbol{u}}{\partial t} + \nabla p = \boldsymbol{F}, \qquad \frac{1}{K(z,\boldsymbol{x})}\frac{\partial p}{\partial t} + \nabla \cdot \boldsymbol{u} = 0, \tag{1}$$

where p is the pressure field, $\boldsymbol{u}$ is the velocity field, ρ is the density of the medium, K is the bulk modulus of the medium, and $(z, \boldsymbol{x}) \in \mathrm{R} \times \mathrm{R}^d$ are the space coordinates. The source is modeled by the forcing term $\boldsymbol{F}$.

We consider in this paper the situation in which a random slab occupies the region

$$\Omega_r = \left\{(z, \boldsymbol{x}),\, \boldsymbol{x} \in \mathrm{R}^d,\, z_i(\boldsymbol{x}) \le z \le 0\right\}$$

and is sandwiched in between two homogeneous half-spaces. The surface $z = 0$ is the top interface and the surface $z = z_i(\boldsymbol{x}) < 0$ is the bottom interface. The medium fluctuations in the region Ω_r vary rapidly in space while the "background" medium is constant. The density of the medium is assumed to be evanescent in the region $z > 0$, which gives pressure release boundary conditions at the top interface. We consider a mismatch at the boundary $z = z_i(\boldsymbol{x})$, which gives jump conditions at the bottom interface. We denote by ρ_0 and K_0 the background medium parameters in the half-space $z \le z_i(\boldsymbol{x})$, and by ρ_1 and K_1 the parameters in the region Ω_r:

$$\frac{1}{K(z, \boldsymbol{x})} = \begin{cases} K_0^{-1} & \text{if } z \le z_i(\boldsymbol{x}), \\ K_1^{-1}\left(1 + \nu_K(z, \boldsymbol{x})\right) & \text{if } z \in (z_i(\boldsymbol{x}), 0), \\ K_1^{-1} & \text{if } z \ge 0, \end{cases}$$

$$\rho(z, \boldsymbol{x}) = \begin{cases} \rho_0 & \text{if } z \le z_i(\boldsymbol{x}), \\ \rho_1 & \text{if } z \in (z_i(\boldsymbol{x}), 0), \\ 0 & \text{if } z \ge 0, \end{cases}$$

where the random field $\nu_K(z, \boldsymbol{x})$ models the medium fluctuations, whose correlation length is l_K.

The source, $\boldsymbol{F}$, is located in the region Ω_r at $z = z_s$, $z_s < 0$, close to the surface $z = 0$ (we will eventually take the limit $z_s \to 0^-$). We shall refer to waves propagating in the direction with a positive z component as up-going waves. The source generates waves that propagate through the random medium and that are reflected by the interface at $z = z_i(\boldsymbol{x})$ and propagate back through the medium. We are interested in the waves that can be recorded at the surface $z = 0$.

The source has the form

$$\boldsymbol{F}(t, z, \boldsymbol{x}) = f_s(t, \boldsymbol{x}) \delta(z - z_s) \boldsymbol{e}_z,$$

where $\boldsymbol{e}_z$ is the unit vector pointing in the z-direction, $z_s < 0$ is the source position. We denote by ω_0 the typical frequency of the source term f_s and by R_0 the diameter of its spatial support (which gives the initial beam width). The typical wavelength associated with the typical frequency ω_0 is $\lambda_0 = 2\pi c_1/\omega_0$, for $c_1 = \sqrt{K_1/\rho_1}$ the background speed in the region Ω_r, which is of the same order as the background speed $c_0 = \sqrt{K_0/\rho_0}$ in the half-space $z \le z_i(\boldsymbol{x})$.

We can now introduce the scaling regime that we consider in this paper:

1) We assume that the correlation length l_K of the medium is much smaller than the typical propagation distance L (of the order of $|z_i|$). We denote by ε^2 the ratio between the correlation length and the typical propagation distance.

2) We assume that the transverse width of the source R_0 and the correlation length of the medium l_K are of the same order. This means that we assume that the ratio R_0/L is of order ε^2. This scaling is motivated by the fact that, in this regime, there is a non-trivial interaction between the fluctuations of the medium and the beam.

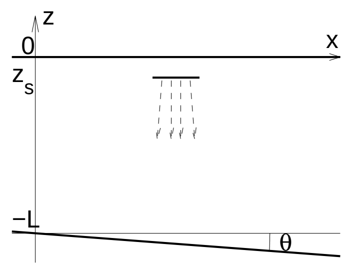

Figure 1. Configuration. The source is located at depth $z_s < 0$ close to the surface. An oblique interface is present at depth $-L$.

3) We assume that the typical wavelength λ_0 is much smaller than the propagation distance L, more precisely, we assume that the ratio λ_0/L is of order ε^4. This high-frequency scaling is motivated by the following considerations. The Rayleigh length for a beam with initial width R_0 and central wavelength λ_0 is of the order of R_0^2/λ_0 in absence of random fluctuations (the Rayleigh length is the distance from beam waist where the beam area is doubled by diffraction). In order to get a Rayleigh length of the order of the propagation distance L, the ratio λ_0/L must be of order ε^4 since $R_0/L \sim \varepsilon^2$.

4) We assume that the distance from the surface $z = 0$ to the source $z = z_s$ is of the order of the wavelength (or smaller), that is, of the order of ε^4.

5) We assume that the bottom interface $z = z_i(\boldsymbol{x})$ is locally flat and its normal vector makes a small angle with respect to $\boldsymbol{e}_z$. The order of magnitude of this angle is of order ε^2, so that Descartes' law predicts that the beam generated by the source and reflected by the interface will be recorded at the surface $z = 0$ with a lateral shift of the order of the radius of the beam. This is the interesting configuration, in which the waves propagate through the same region of the random medium. Furthermore, the pressure release boundary conditions also reflect the waves, so they will experience several round trips between the two interfaces $z = 0$ and $z = z_i(\boldsymbol{x})$.

Henceforth we shall assume non-dimensionalized units chosen such the background bulk modulus K_1 and density ρ_1 in the region Ω_r are one, hence, the background speed $c_1 = \sqrt{K_1/\rho_1}$ and impedance $Z_1 = \sqrt{K_1\rho_1}$ are also equal to one. If we consider the propagation distance, L, as our reference distance of order one in this scaled regime, then
1) the equation of the bottom interface is $z = -L - \varepsilon^2\boldsymbol{\theta}\cdot\boldsymbol{x}$ where $\boldsymbol{\theta} \in \mathrm{R}^d$ with $|\boldsymbol{\theta}| = 1$ and $L > 0$ is the depth of the interface,
2) the source is localized at $z = -\varepsilon^4 z_0$ and it has the form

$$\boldsymbol{F}(t,z,\boldsymbol{x}) = f\Big(\frac{t}{\varepsilon^4},\frac{\boldsymbol{x}}{\varepsilon^2}\Big)\delta\big(z+\varepsilon^4 z_0\big)\boldsymbol{e}_z, \tag{2}$$

where $z_0 > 0$ and $f(t,\boldsymbol{x})$ is the normalized source shape function (with time and spatial scales of variations of order one),

3) the medium fluctuations have the form

$$\frac{1}{K(z,\boldsymbol{x})} = \begin{cases} K_0^{-1} & \text{if } z \le -L - \varepsilon^2 \boldsymbol{\theta}\cdot\boldsymbol{x}, \\ 1 + \varepsilon^3 \nu(\frac{z}{\varepsilon^2}, \frac{\boldsymbol{x}}{\varepsilon^2}) & \text{if } z \in (-L - \varepsilon^2 \boldsymbol{\theta}\cdot\boldsymbol{x}, 0), \\ 1 & \text{if } z \ge 0, \end{cases}$$

$$\rho(z,\boldsymbol{x}) = \begin{cases} \rho_0 & \text{if } z \le -L - \varepsilon^2 \boldsymbol{\theta}\cdot\boldsymbol{x}, \\ 1 & \text{if } z \in (-L - \varepsilon^2 \boldsymbol{\theta}\cdot\boldsymbol{x}, 0), \\ 0 & \text{if } z \ge 0, \end{cases}$$

where the zero-mean, stationary random field ν has a correlation length of order one and standard deviation of order one, see Figure 1. We also assume that it satisfies strong mixing conditions in z. Here the amplitude ε^3 of the fluctuations has been chosen so as to obtain an effective regime of order one when ε goes to zero. That is, if the magnitude of the fluctuations is smaller than ε^3, then the wave would propagate as if the medium was homogeneous, while if the order of magnitude is larger, then the wave would not penetrate the slab down to the bottom interface. The scaling that we consider here corresponds to the physically most interesting situation.

3. The Boundary Value Problem

Since both the medium and the source have transverse spatial variations at the scale ε^2, it is convenient to rescale the transverse variable $\boldsymbol{x}/\varepsilon^2 \to \boldsymbol{x}$ and to introduce the rescaled fields $\boldsymbol{u}^\varepsilon$ and p^ε:

$$\boldsymbol{u}^\varepsilon(t,z,\boldsymbol{x}) = \boldsymbol{u}(t, z - \varepsilon^4 \boldsymbol{\theta}\cdot\boldsymbol{x}, \varepsilon^2 \boldsymbol{x}), \quad p^\varepsilon(t,z,\boldsymbol{x}) = p(t, z - \varepsilon^4 \boldsymbol{\theta}\cdot\boldsymbol{x}, \varepsilon^2 \boldsymbol{x}). \tag{3}$$

In this new frame, the bottom interface is $z = -L$ while the top surface is $z = \varepsilon^4 \boldsymbol{\theta}\cdot\boldsymbol{x}$.

In the region Ω_r the fields satisfy

$$\frac{\partial \boldsymbol{u}^\varepsilon}{\partial t} + \begin{bmatrix} \partial_z \\ \varepsilon^2 \boldsymbol{\theta}\partial_z + \varepsilon^{-2}\nabla_{\boldsymbol{x}} \end{bmatrix} p^\varepsilon = f\Big(\frac{t}{\varepsilon^4}, \boldsymbol{x}\Big)\delta\big(z + \varepsilon^4(z_0 - \boldsymbol{\theta}\cdot\boldsymbol{x})\big) \begin{bmatrix} 1 \\ \boldsymbol{0} \end{bmatrix}, \tag{4}$$

$$\Big(1 + \varepsilon^3 \nu\big(\frac{z}{\varepsilon^2} - \varepsilon^2 \boldsymbol{\theta}\cdot\boldsymbol{x}, \boldsymbol{x}\big)\Big) \frac{\partial p^\varepsilon}{\partial t} + \begin{bmatrix} \partial_z \\ \varepsilon^2 \boldsymbol{\theta}\partial_z + \varepsilon^{-2}\nabla_{\boldsymbol{x}} \end{bmatrix} \cdot \boldsymbol{u}^\varepsilon = 0, \tag{5}$$

where $\nabla_{\boldsymbol{x}}$ stands for the gradient with respect to the transverse spatial variables $\boldsymbol{x}$. The pressure field and its z-derivative in the region Ω_r can be written as:

$$p^\varepsilon(t,z,\boldsymbol{x}) = \frac{1}{2\pi}\int \Big(\widetilde{a}^\varepsilon(k,z,\boldsymbol{x}) e^{ik\frac{z}{\varepsilon^4}} + \widetilde{b}^\varepsilon(k,z,\boldsymbol{x}) e^{-ik\frac{z}{\varepsilon^4}}\Big) e^{-ik\frac{t}{\varepsilon^4}} dk,$$

$$\frac{\partial p^\varepsilon}{\partial z}(t,z,\boldsymbol{x}) = \frac{1}{2\pi}\int \frac{ik}{\varepsilon^4}\Big(\widetilde{a}^\varepsilon(k,z,\boldsymbol{x}) e^{ik\frac{z}{\varepsilon^4}} - \widetilde{b}^\varepsilon(k,z,\boldsymbol{x}) e^{-ik\frac{z}{\varepsilon^4}}\Big) e^{-ik\frac{t}{\varepsilon^4}} dk,$$

with the complex amplitudes $\widetilde{a}^\varepsilon$ and $\widetilde{b}^\varepsilon$ of the up- and down-propagating modes given explicitly by

$$\widetilde{a}^\varepsilon(k,z,\boldsymbol{x}) = \frac{1}{2}\Big[\int \Big(\frac{1}{\varepsilon^4} p^\varepsilon(t,z,\boldsymbol{x}) + \frac{1}{ik}\frac{\partial p^\varepsilon}{\partial z}(t,z,\boldsymbol{x})\Big) e^{ik\frac{t}{\varepsilon^4}} dt\Big] e^{-ik\frac{z}{\varepsilon^4}},$$

$$\widetilde{b}^\varepsilon(k,z,\boldsymbol{x}) = \frac{1}{2}\Big[\int \Big(\frac{1}{\varepsilon^4} p^\varepsilon(t,z,\boldsymbol{x}) - \frac{1}{ik}\frac{\partial p^\varepsilon}{\partial z}(t,z,\boldsymbol{x})\Big) e^{ik\frac{t}{\varepsilon^4}} dt\Big] e^{ik\frac{z}{\varepsilon^4}}.$$

The pressure release boundary conditions impose $p^\varepsilon(t, z = \varepsilon^4 \boldsymbol{\theta} \cdot \boldsymbol{x}, \boldsymbol{x}) = 0$.

Using (4-5) we obtain the following mode coupling equations

$$\frac{\partial \widetilde{a}^\varepsilon}{\partial z} = \left(\frac{ik}{2\varepsilon} \nu\Big(\frac{z}{\varepsilon^2}, \boldsymbol{x}\Big) + \frac{i}{2k} \Delta_{\boldsymbol{x}} \right) \widetilde{a}^\varepsilon + e^{-2ik\frac{z}{\varepsilon^4}} \left(\frac{ik}{2\varepsilon} \nu\Big(\frac{z}{\varepsilon^2}, \boldsymbol{x}\Big) + \frac{i}{2k} \Delta_{\boldsymbol{x}} \right) \widetilde{b}^\varepsilon, \quad (6)$$

$$\frac{\partial \widetilde{b}^\varepsilon}{\partial z} = -e^{2ik\frac{z}{\varepsilon^4}} \left(\frac{ik}{2\varepsilon} \nu\Big(\frac{z}{\varepsilon^2}, \boldsymbol{x}\Big) + \frac{i}{2k} \Delta_{\boldsymbol{x}} \right) \widetilde{a}^\varepsilon - \left(\frac{ik}{2\varepsilon} \nu\Big(\frac{z}{\varepsilon^2}, \boldsymbol{x}\Big) + \frac{i}{2k} \Delta_{\boldsymbol{x}} \right) \widetilde{b}^\varepsilon, \quad (7)$$

where we have neglected terms of order ε^2. Note that the z-derivatives of $\widetilde{a}^\varepsilon$ and $\widetilde{b}^\varepsilon$ are of the order of ε^{-1}, so we have to leading order $\widetilde{a}^\varepsilon(k, z, \boldsymbol{x}) = \widetilde{a}^\varepsilon(k, 0^+, \boldsymbol{x})$ and $\widetilde{b}^\varepsilon(k, z, \boldsymbol{x}) = \widetilde{b}^\varepsilon(k, 0^+, \boldsymbol{x})$ for $z \in (-\varepsilon^4 z_0 + \varepsilon^4 \boldsymbol{\theta} \cdot \boldsymbol{x}, \varepsilon^4 \boldsymbol{\theta} \cdot \boldsymbol{x})$ (the region between the source and the top surface), and we denote by $\widetilde{a}^\varepsilon(k, 0^-, \boldsymbol{x})$ and $\widetilde{b}^\varepsilon(k, 0^-, \boldsymbol{x})$ the values of $\widetilde{a}^\varepsilon(k, z, \boldsymbol{x})$ and $\widetilde{b}^\varepsilon(k, z, \boldsymbol{x})$ just below the source.

The system (6-7) is valid in $z \in (-L, 0)$ and it is complemented with the following boundary and jump conditions at $z = 0^+$ (the top interface), $z = 0^-$ (the source) and $z = -L$ (the bottom interface):

$$\widetilde{a}^\varepsilon(k, 0^+, \boldsymbol{x}) e^{ik\boldsymbol{\theta}\cdot\boldsymbol{x}} + \widetilde{b}^\varepsilon(k, 0^+, \boldsymbol{x}) e^{-ik\boldsymbol{\theta}\cdot\boldsymbol{x}} = 0, \quad (8)$$

$$\begin{aligned} &\big[\widetilde{a}^\varepsilon(k, 0^+, \boldsymbol{x}) e^{-ik(z_0 - \boldsymbol{\theta}\cdot\boldsymbol{x})} + \widetilde{b}^\varepsilon(k, 0^+, \boldsymbol{x}) e^{ik(z_0 - \boldsymbol{\theta}\cdot\boldsymbol{x})}\big] \\ &\quad - \big[\widetilde{a}^\varepsilon(k, 0^-, \boldsymbol{x}) e^{-ik(z_0 - \boldsymbol{\theta}\cdot\boldsymbol{x})} + \widetilde{b}^\varepsilon(k, 0^-, \boldsymbol{x}) e^{ik(z_0 - \boldsymbol{\theta}\cdot\boldsymbol{x})}\big] = \widetilde{f}(k, \boldsymbol{x}), \end{aligned} \quad (9)$$

$$\begin{aligned} &\big[\widetilde{a}^\varepsilon(k, 0^+, \boldsymbol{x}) e^{-ik(z_0 - \boldsymbol{\theta}\cdot\boldsymbol{x})} - \widetilde{b}^\varepsilon(k, 0^+, \boldsymbol{x}) e^{ik(z_0 - \boldsymbol{\theta}\cdot\boldsymbol{x})}\big] \\ &\quad - \big[\widetilde{a}^\varepsilon(k, 0^-, \boldsymbol{x}) e^{-ik(z_0 - \boldsymbol{\theta}\cdot\boldsymbol{x})} - \widetilde{b}^\varepsilon(k, 0^-, \boldsymbol{x}) e^{ik(z_0 - \boldsymbol{\theta}\cdot\boldsymbol{x})}\big] = 0, \end{aligned} \quad (10)$$

$$\widetilde{a}^\varepsilon(k, -L, \boldsymbol{x}) e^{-ik\frac{L}{\varepsilon^4}} - \mathcal{R}_0 \widetilde{b}^\varepsilon(k, -L, \boldsymbol{x}) e^{ik\frac{L}{\varepsilon^4}} = 0, \quad (11)$$

where $\mathcal{R}_0 = (Z_0 - 1)/(Z_0 + 1)$ is the reflection coefficient of the bottom interface, $Z_0 = \sqrt{K_0 \rho_0}$ is the impedance of the bottom homogeneous half-space, and the Fourier transforms are defined by

$$\widetilde{f}(k, \boldsymbol{x}) = \int f(t, \boldsymbol{x}) e^{ikt} dt, \quad \hat{f}(k, \boldsymbol{\kappa}) = \int \widetilde{f}(k, \boldsymbol{x}) e^{-i\boldsymbol{\kappa}\cdot\boldsymbol{x}} d\boldsymbol{x}. \quad (12)$$

We simplify the condition (9) by taking $z_0 \to 0$ (which means that the distance from the source to the right interface is smaller than the wavelength), and we find that the system (6-7) in $z \in (-L, 0)$ is complemented with the boundary conditions (11) at $z = -L$ and

$$\widetilde{b}^\varepsilon(k, 0^-, \boldsymbol{x}) + \widetilde{a}^\varepsilon(k, 0^-, \boldsymbol{x}) e^{2ik\boldsymbol{\theta}\cdot\boldsymbol{x}} = -\widetilde{f}(k, \boldsymbol{x}) e^{ik\boldsymbol{\theta}\cdot\boldsymbol{x}}, \quad (13)$$

at $z = 0^-$. The waves that can be observed at the surface $z = 0^+$ are given by

$$\widetilde{a}^\varepsilon(k, 0^+, \boldsymbol{x}) = \frac{1}{2} \widetilde{a}^\varepsilon(k, 0^-, \boldsymbol{x}) - \frac{1}{2} \widetilde{b}^\varepsilon(k, 0^-, \boldsymbol{x}) e^{-2ik\boldsymbol{\theta}\cdot\boldsymbol{x}}, \quad (14)$$

$$\widetilde{b}^\varepsilon(k, 0^+, \boldsymbol{x}) = -\frac{1}{2} \widetilde{a}^\varepsilon(k, 0^-, \boldsymbol{x}) e^{2ik\boldsymbol{\theta}\cdot\boldsymbol{x}} + \frac{1}{2} \widetilde{b}^\varepsilon(k, 0^-, \boldsymbol{x}). \quad (15)$$

The signals recorded at the surface are in practice the vertical velocity (normal to the top surface) defined by

$$v^\varepsilon(t,\boldsymbol{x}) := \boldsymbol{e}_z \cdot \boldsymbol{u}(t,0,\varepsilon^2\boldsymbol{x}), \tag{16}$$

which is such that

$$\frac{\partial v^\varepsilon}{\partial t}(t,\boldsymbol{x}) = -\frac{\partial p^\varepsilon}{\partial z}(t,\varepsilon^4\boldsymbol{\theta}\cdot\boldsymbol{x},\boldsymbol{x}).$$

Therefore

$$v^\varepsilon(t,\boldsymbol{x}) = \frac{1}{2\pi}\int \left(\widetilde{a}^\varepsilon(k,0^+,\boldsymbol{x})e^{ik\boldsymbol{\theta}\cdot\boldsymbol{x}} - \widetilde{b}^\varepsilon(k,0^+,\boldsymbol{x})e^{-ik\boldsymbol{\theta}\cdot\boldsymbol{x}}\right) e^{-ik\frac{t}{\varepsilon^4}}dk. \tag{17}$$

4. The Reflection Operator

We define the lateral Fourier modes

$$\hat{a}^\varepsilon(k,z,\boldsymbol{\kappa}) = \int \widetilde{a}^\varepsilon(k,z,\boldsymbol{x})e^{-i\boldsymbol{\kappa}\cdot\boldsymbol{x}}d\boldsymbol{x}, \quad \hat{b}^\varepsilon(k,z,\boldsymbol{\kappa}) = \int \widetilde{b}^\varepsilon(k,z,\boldsymbol{x})e^{-i\boldsymbol{\kappa}\cdot\boldsymbol{x}}d\boldsymbol{x}. \tag{18}$$

They satisfy for $z \in (-L,0)$

$$\begin{aligned}
\frac{d\hat{a}^\varepsilon}{dz}(k,z,\boldsymbol{\kappa}) &= \int \widehat{\boldsymbol{\mathcal{L}}}^\varepsilon\left(k,z,\boldsymbol{\kappa},\boldsymbol{\kappa}'\right)\hat{a}^\varepsilon(k,z,\boldsymbol{\kappa}')d\boldsymbol{\kappa}' \\
&\quad + e^{-\frac{2ikz}{\varepsilon^4}}\int \widehat{\boldsymbol{\mathcal{L}}}^\varepsilon\left(k,z,\boldsymbol{\kappa},\boldsymbol{\kappa}'\right)\hat{b}^\varepsilon(k,z,\boldsymbol{\kappa}')d\boldsymbol{\kappa}', \\
\frac{d\hat{b}^\varepsilon}{dz}(k,z,\boldsymbol{\kappa}) &= -e^{-\frac{2ikz}{\varepsilon^4}}\int \widehat{\boldsymbol{\mathcal{L}}}^\varepsilon\left(k,z,\boldsymbol{\kappa},\boldsymbol{\kappa}'\right)\hat{a}^\varepsilon(k,z,\boldsymbol{\kappa}')d\boldsymbol{\kappa}' \\
&\quad - \int \widehat{\boldsymbol{\mathcal{L}}}^\varepsilon\left(k,z,\boldsymbol{\kappa},\boldsymbol{\kappa}'\right)\hat{b}^\varepsilon(k,z,\boldsymbol{\kappa}')d\boldsymbol{\kappa}',
\end{aligned}$$

where we have defined

$$\widehat{\boldsymbol{\mathcal{L}}}^\varepsilon\left(k,z,\boldsymbol{\kappa}_1,\boldsymbol{\kappa}_2\right) = -\frac{i}{2k}|\boldsymbol{\kappa}_1|^2\delta(\boldsymbol{\kappa}_1-\boldsymbol{\kappa}_2) + \frac{ik}{2(2\pi)^d\varepsilon}\hat{\nu}\Big(\frac{z}{\varepsilon^2},\boldsymbol{\kappa}_1-\boldsymbol{\kappa}_2\Big), \tag{19}$$

with $\hat{\nu}(z,\boldsymbol{\kappa})$ the partial Fourier transform (in $\boldsymbol{x}$) of $\nu(z,\boldsymbol{x})$. The boundary conditions (11) and 13) at $z=-L$ and $z=0^-$ read

$$\hat{a}^\varepsilon(k,-L,\boldsymbol{\kappa})e^{-ik\frac{L}{\varepsilon^4}} - \mathcal{R}_0\hat{b}^\varepsilon(k,-L,\boldsymbol{\kappa})e^{ik\frac{L}{\varepsilon^4}} = 0, \tag{20}$$

$$\hat{b}^\varepsilon(k,0^-,\boldsymbol{\kappa}) + \hat{a}^\varepsilon(k,0^-,\boldsymbol{\kappa}-2k\boldsymbol{\theta}) = -\hat{f}(k,\boldsymbol{\kappa}-k\boldsymbol{\theta}). \tag{21}$$

We now apply an invariant imbedding technique to obtain that

$$\hat{b}^\varepsilon(k,-L,\boldsymbol{\kappa}) = \int \widehat{\boldsymbol{\mathcal{T}}}^\varepsilon(k,z,\boldsymbol{\kappa},\boldsymbol{\kappa}')\hat{b}^\varepsilon(k,z,\boldsymbol{\kappa}')d\boldsymbol{\kappa}', \tag{22}$$

$$\hat{a}^\varepsilon(k,z,\boldsymbol{\kappa}) = e^{2ik\frac{L}{\varepsilon^4}}\int \widehat{\boldsymbol{\mathcal{R}}}^\varepsilon(k,z,\boldsymbol{\kappa},\boldsymbol{\kappa}')\hat{b}^\varepsilon(k,z,\boldsymbol{\kappa}')d\boldsymbol{\kappa}', \tag{23}$$

where the kernels of the operators $\widehat{\boldsymbol{\mathcal{T}}}^\varepsilon$ and $\widehat{\boldsymbol{\mathcal{R}}}^\varepsilon$ satisfy

$$
\begin{aligned}
&\frac{d}{dz}\widehat{\boldsymbol{\mathcal{R}}}^\varepsilon(k,z,\boldsymbol{\kappa},\boldsymbol{\kappa}') = e^{-\frac{2ik(z+L)}{\varepsilon^4}}\widehat{\boldsymbol{\mathcal{L}}}^\varepsilon\left(k,z,\boldsymbol{\kappa},\boldsymbol{\kappa}'\right) \\
&\quad + \int \widehat{\boldsymbol{\mathcal{L}}}^\varepsilon(k,z,\boldsymbol{\kappa},\boldsymbol{\kappa}_1)\widehat{\boldsymbol{\mathcal{R}}}^\varepsilon(k,z,\boldsymbol{\kappa}_1,\boldsymbol{\kappa}')d\boldsymbol{\kappa}_1 + \int \widehat{\boldsymbol{\mathcal{R}}}^\varepsilon(k,z,\boldsymbol{\kappa},\boldsymbol{\kappa}_1)\widehat{\boldsymbol{\mathcal{L}}}^\varepsilon\left(k,z,\boldsymbol{\kappa}_1,\boldsymbol{\kappa}'\right)d\boldsymbol{\kappa}_1 \\
&\quad + e^{\frac{2ik(z+L)}{\varepsilon^4}}\iint \widehat{\boldsymbol{\mathcal{R}}}^\varepsilon(k,z,\boldsymbol{\kappa},\boldsymbol{\kappa}_1)\widehat{\boldsymbol{\mathcal{L}}}^\varepsilon(k,z,\boldsymbol{\kappa}_1,\boldsymbol{\kappa}_2)\widehat{\boldsymbol{\mathcal{R}}}^\varepsilon(k,z,\boldsymbol{\kappa}_2,\boldsymbol{\kappa}')\,d\boldsymbol{\kappa}_1 d\boldsymbol{\kappa}_2, \qquad (24) \\
&\frac{d}{dz}\widehat{\boldsymbol{\mathcal{T}}}^\varepsilon(k,z,\boldsymbol{\kappa},\boldsymbol{\kappa}') = \int \widehat{\boldsymbol{\mathcal{T}}}^\varepsilon(k,z,\boldsymbol{\kappa},\boldsymbol{\kappa}_1)\widehat{\boldsymbol{\mathcal{L}}}^\varepsilon\left(k,z,\boldsymbol{\kappa}_1,\boldsymbol{\kappa}'\right)d\boldsymbol{\kappa}_1 \\
&\quad + e^{\frac{2ik(z+L)}{\varepsilon^4}}\iint \widehat{\boldsymbol{\mathcal{T}}}^\varepsilon(k,z,\boldsymbol{\kappa},\boldsymbol{\kappa}_1)\widehat{\boldsymbol{\mathcal{L}}}^\varepsilon(k,z,\boldsymbol{\kappa}_1,\boldsymbol{\kappa}_2)\widehat{\boldsymbol{\mathcal{R}}}^\varepsilon(k,z,\boldsymbol{\kappa}_2,\boldsymbol{\kappa}')\,d\boldsymbol{\kappa}_1 d\boldsymbol{\kappa}_2. \qquad (25)
\end{aligned}
$$

This system is complemented with the initial conditions at $z=-L$, which are obtained from (20):

$$
\widehat{\boldsymbol{\mathcal{R}}}^\varepsilon(k,-L,\boldsymbol{\kappa},\boldsymbol{\kappa}') = \mathcal{R}_0\delta(\boldsymbol{\kappa}-\boldsymbol{\kappa}'), \quad \widehat{\boldsymbol{\mathcal{T}}}^\varepsilon(k,-L,\boldsymbol{\kappa},\boldsymbol{\kappa}') = \delta(\boldsymbol{\kappa}-\boldsymbol{\kappa}').
$$

The transmission and reflection operators evaluated at $z=0^-$ carry all the relevant information about the random medium from the point of view of the transmitted and reflected waves.

Using (21) and (23) we find

$$
\hat{b}^\varepsilon(k,0^-,\boldsymbol{\kappa}) = -\hat{f}(k,\boldsymbol{\kappa}-k\boldsymbol{\theta}) - e^{2ik\frac{L}{\varepsilon^4}}\int \widehat{\boldsymbol{\mathcal{R}}}^\varepsilon(k,0,\boldsymbol{\kappa}-2k\boldsymbol{\theta},\boldsymbol{\kappa}')\hat{b}^\varepsilon(k,0^-,\boldsymbol{\kappa}')d\boldsymbol{\kappa}'.
$$

The solution of this equation can be expanded as a series:

$$
\begin{aligned}
&\hat{b}^\varepsilon(k,0^-,\boldsymbol{\kappa}) = -\hat{f}(k,\boldsymbol{\kappa}-k\boldsymbol{\theta}) + e^{2ik\frac{L}{\varepsilon^4}}\int \widehat{\boldsymbol{\mathcal{R}}}^\varepsilon(k,0,\boldsymbol{\kappa}-2k\boldsymbol{\theta},\boldsymbol{\kappa}_1+k\boldsymbol{\theta})\hat{f}(k,\boldsymbol{\kappa}_1)d\boldsymbol{\kappa}_1 \\
&\quad - e^{4ik\frac{L}{\varepsilon^4}}\int \widehat{\boldsymbol{\mathcal{R}}}^\varepsilon(k,0,\boldsymbol{\kappa}-2k\boldsymbol{\theta},\boldsymbol{\kappa}_1+k\boldsymbol{\theta})\widehat{\boldsymbol{\mathcal{R}}}^\varepsilon(k,0,\boldsymbol{\kappa}_1-k\boldsymbol{\theta},\boldsymbol{\kappa}_2+k\boldsymbol{\theta})\hat{f}(k,\boldsymbol{\kappa}_2)d\boldsymbol{\kappa}_1 d\boldsymbol{\kappa}_2 \\
&\quad + e^{6ik\frac{L}{\varepsilon^4}}\cdots, \\
&\hat{a}^\varepsilon(k,0^-,\boldsymbol{\kappa}) = -\hat{f}(k,\boldsymbol{\kappa}+k\boldsymbol{\theta}) - \hat{b}^\varepsilon(k,0^-,\boldsymbol{\kappa}+2k\boldsymbol{\theta}),
\end{aligned}
$$

and therefore

$$
\begin{aligned}
&\hat{b}^\varepsilon(k,0^+,\boldsymbol{\kappa}) = \hat{b}^\varepsilon(k,0^-,\boldsymbol{\kappa}) + \frac{1}{2}\hat{f}(k,\boldsymbol{\kappa}-k\boldsymbol{\theta}), \\
&\hat{a}^\varepsilon(k,0^+,\boldsymbol{\kappa}) = \hat{a}^\varepsilon(k,0^-,\boldsymbol{\kappa}) + \frac{1}{2}\hat{f}(k,\boldsymbol{\kappa}+k\boldsymbol{\theta}), \\
&\hat{a}^\varepsilon(k,0^+,\boldsymbol{\kappa}-k\boldsymbol{\theta}) - \hat{b}^\varepsilon(k,0^+,\boldsymbol{\kappa}+k\boldsymbol{\theta}) = \hat{f}(k,\boldsymbol{\kappa}) \\
&\quad - e^{2ik\frac{L}{\varepsilon^4}}\int \widehat{\boldsymbol{\mathcal{R}}}^\varepsilon(k,0,\boldsymbol{\kappa}-k\boldsymbol{\theta},\boldsymbol{\kappa}_1+k\boldsymbol{\theta})\hat{f}(k,\boldsymbol{\kappa}_1)d\boldsymbol{\kappa}_1 \\
&\quad + e^{4ik\frac{L}{\varepsilon^4}}\int \widehat{\boldsymbol{\mathcal{R}}}^\varepsilon(k,0,\boldsymbol{\kappa}-k\boldsymbol{\theta},\boldsymbol{\kappa}_1+k\boldsymbol{\theta})\widehat{\boldsymbol{\mathcal{R}}}^\varepsilon(k,0,\boldsymbol{\kappa}_1-k\boldsymbol{\theta},\boldsymbol{\kappa}_2+k\boldsymbol{\theta})\hat{f}(k,\boldsymbol{\kappa}_2)d\boldsymbol{\kappa}_1 d\boldsymbol{\kappa}_2 \\
&\quad + e^{6ik\frac{L}{\varepsilon^4}}\cdots. \qquad (26)
\end{aligned}
$$

Our objective in the next section is to characterize the reflected vertical velocity field (17) around the sequence of expected arrival times $2jL$ (which is j times the round trip time from the surface to the bottom interface):

$$\begin{aligned} v_j^\varepsilon(s,\boldsymbol{x}) &:= v^\varepsilon(2jL+\varepsilon^4 s,\boldsymbol{x}) \\ &= \frac{1}{(2\pi)^{d+1}}\iint \left[\hat{a}^\varepsilon(k,0^+,\boldsymbol{\kappa}-k\boldsymbol{\theta})-\hat{b}^\varepsilon(k,0^+,\boldsymbol{\kappa}+k\boldsymbol{\theta})\right] \\ &\qquad \times e^{i(\boldsymbol{\kappa}\cdot\boldsymbol{x}-ks)}e^{-2ijk\frac{L}{\varepsilon^4}}d\boldsymbol{\kappa}dk. \end{aligned} \tag{27}$$

We can see that the presence of the rapid phase in (27) will select the term with the opposite rapid phase in the sum (26) in the limit $\varepsilon\to 0$. We write the kernel of the reflection operator in spatial coordinates via

$$\widetilde{\boldsymbol{\mathcal{R}}}^\varepsilon(k,z,\boldsymbol{x},\boldsymbol{x}') = \frac{1}{(2\pi)^d}\iint e^{i(\boldsymbol{x}\cdot\boldsymbol{\kappa}-\boldsymbol{x}'\cdot\boldsymbol{\kappa}')}\widehat{\boldsymbol{\mathcal{R}}}^\varepsilon(k,z,\boldsymbol{\kappa},\boldsymbol{\kappa}')d\boldsymbol{\kappa}d\boldsymbol{\kappa}', \tag{28}$$

and will in the next section discuss an “effective” scaling limit representation of this, in the sense that it is a representation that gives the correct statistics for the reflected wave field.

5. The Asymptotic Representation of the Reflected Field

We consider the reflected fields v_j^ε defined by (27) and use diffusion approximation theorems to identify a limit random Schrödinger model. The main result is the following one.

Proposition 5.1: *For all j, the processes $(v_j^\varepsilon(s,\boldsymbol{x}))_{s\in\mathrm{R},\boldsymbol{x}\in\mathrm{R}^d}$ converge in distribution as $\varepsilon\to 0$ in the space $C^0(\mathrm{R},L^2(\mathrm{R}^d,\mathrm{R}^2))\cap L^2(\mathrm{R},L^2(\mathrm{R}^d,\mathrm{R}^2))$ to the limit process $(v_j(s,\boldsymbol{x}))_{s\in\mathrm{R},\boldsymbol{x}\in\mathrm{R}^d}$. We have in particular*

$$v_0(s,\boldsymbol{x}) = \frac{1}{2\pi}\int \widetilde{f}(k,\boldsymbol{x})e^{-iks}dk, \tag{29}$$

$$v_1(s,\boldsymbol{x}) = -\frac{1}{2\pi}\iint \widetilde{\boldsymbol{\mathcal{R}}}(k,0,\boldsymbol{x},\boldsymbol{x}')e^{ik\boldsymbol{\theta}\cdot\boldsymbol{x}+ik\boldsymbol{\theta}\cdot\boldsymbol{x}'}\widetilde{f}(k,\boldsymbol{x}')d\boldsymbol{x}'e^{-iks}dk, \tag{30}$$

$$\begin{aligned} v_2(s,\boldsymbol{x}) &= \frac{1}{2\pi}\iiint \widetilde{\boldsymbol{\mathcal{R}}}(k,0,\boldsymbol{x},\boldsymbol{x}')\widetilde{\boldsymbol{\mathcal{R}}}(k,0,\boldsymbol{x}',\boldsymbol{x}'')e^{ik\boldsymbol{\theta}\cdot\boldsymbol{x}+2ik\boldsymbol{\theta}\cdot\boldsymbol{x}'+ik\boldsymbol{\theta}\cdot\boldsymbol{x}''} \\ &\qquad \times\widetilde{f}(k,\boldsymbol{x}'')d\boldsymbol{x}'d\boldsymbol{x}''e^{-iks}dk. \end{aligned} \tag{31}$$

Here $C^0(\mathrm{R},L^2(\mathrm{R}^d,\mathrm{R}^2))$ is the space of continuous functions (in s) with values in $L^2(\mathrm{R}^d,\mathrm{R}^2)$ and $L^2(\mathrm{R},L^2(\mathrm{R}^d,\mathrm{R}^2)) = L^2(\mathrm{R}\times\mathrm{R}^d,\mathrm{R}^2)$. The kernel of the operator $\widetilde{\boldsymbol{\mathcal{R}}}(k,z,\boldsymbol{x},\boldsymbol{x}')$ is the solution of the following Itô-Schrödinger model

$$\begin{aligned} d\widetilde{\boldsymbol{\mathcal{R}}}(k,z,\boldsymbol{x},\boldsymbol{x}') &= \frac{i}{2k}\left(\Delta_{\boldsymbol{x}}+\Delta_{\boldsymbol{x}'}\right)\widetilde{\boldsymbol{\mathcal{R}}}(k,z,\boldsymbol{x},\boldsymbol{x}')\,dz \\ &\quad +\frac{ik}{2}\widetilde{\boldsymbol{\mathcal{R}}}(k,z,\boldsymbol{x},\boldsymbol{x}')\circ\left(dB(z,\boldsymbol{x})+dB(z,\boldsymbol{x}')\right), \end{aligned} \tag{32}$$

with the initial condition at $z=-L$:

$$\widetilde{\boldsymbol{\mathcal{R}}}(k,-L,\boldsymbol{x},\boldsymbol{x}') = \mathcal{R}_0\delta(\boldsymbol{x}-\boldsymbol{x}').$$

The symbol $\circ$ *stands for the Stratonovich stochastic integral,* $B(z,\boldsymbol{x})$ *is a real-valued Brownian field with covariance*

$$\mathrm{E}[B(z_1,\boldsymbol{x}_1)B(z_2,\boldsymbol{x}_2)] = \min\{z_1,z_2\}D(\boldsymbol{x}_1-\boldsymbol{x}_2), \tag{33}$$

and we have used the notations

$$C(z,\boldsymbol{x}) = \mathrm{E}[\nu(z'+z,\boldsymbol{x}'+\boldsymbol{x})\nu(z',\boldsymbol{x}')], \tag{34}$$

$$D(\boldsymbol{x}) = \int_{-\infty}^{\infty} C(z,\boldsymbol{x})dz. \tag{35}$$

The moments of the finite-dimensional distributions also converge, in the sense that

$$\mathrm{E}\Big[\prod_{l=1}^{q} v_j^{\varepsilon}(s_l,\boldsymbol{x}_l)^{m_l}\Big] \stackrel{\varepsilon\to 0}{\longrightarrow} \mathrm{E}\Big[\prod_{l=1}^{q} v_j(s_l,\boldsymbol{x}_l)^{m_l}\Big], \tag{36}$$

for any $q\in\mathrm{N}$, $(s_l)_{l=1,\dots,q}\in\mathrm{R}^q$, $(\boldsymbol{x}_l)_{l=1,\dots,q}\in\mathrm{R}^{dq}$, *and* $(m_l)_{l=1,\dots,q}\in\mathrm{N}^q$.

Note that

$$v_0(s,\boldsymbol{x}) = f(s,\boldsymbol{x})$$

is the field directly emitted upward by the source to the surface, while $v_1(s,\boldsymbol{x})$ is the field emitted downward by the source and that has been reflected once by the bottom interface. The fields v_j, $j\geq 2$ are the multiples that have been reflected j times by the bottom surface and by the top surface.

The statistical properties of the operator $\widetilde{\boldsymbol{\mathcal{R}}}$ have been studied in [6]. Therefore we can use the results contained in that paper in order to analyze the statistical properties of the recorded vertical velocity field.

6. Homogeneous Medium

If the medium is homogeneous, then

$$\widetilde{\boldsymbol{\mathcal{R}}}(k,0,\boldsymbol{x},\boldsymbol{x}') = \mathcal{R}_0\Big(\frac{k}{4\pi L}\Big)^{d/2} e^{-i\frac{\pi d}{4}} \exp\Big(-i\frac{k|\boldsymbol{x}-\boldsymbol{x}'|^2}{4L}\Big).$$

Let us assume that the source has the form

$$f(t,\boldsymbol{x}) = f_0(t)e^{-ik_0 t}\exp\Big(-\frac{|\boldsymbol{x}|^2}{2r_0^2}\Big),$$

and that the bandwidth of $f_0(t)$ is smaller than the carrier frequency k_0. Then

$$|v_1(t,\boldsymbol{x})|^2 = \mathcal{R}_0^2\Big(1+\frac{4L^2}{k_0^2 r_0^4}\Big)^{-d}|f_0(t)|^2\exp\Big(-\frac{|\boldsymbol{x}+2\boldsymbol{\theta}L|^2}{r_0^2\big(1+\frac{4L^2}{k_0^2r_0^4}\big)}\Big). \tag{37}$$

The classical diffraction spreading due to the round trip from the surface to the bottom interface and the shift of the envelope of the beam due to the small tilt $\boldsymbol{\theta}$ of the bottom interface are noticeable.

7. Random Medium

In this section we state the assumptions regarding the random medium that allow us to get convenient and explicit expressions for some quantities of interest. We remark that the essential scaling assumptions are the scaling of the source, the medium fluctuations and the travel time in terms of the small parameter ε as described in Section 2. Here, we make some subsequent scaling assumptions that are useful to evaluate the expressions deriving from Proposition 5.1 and we specify in the next section the results and assumptions.

We assume that

(a) the pulse has carrier frequency k_0 and it is narrowband,
(b) the input beam spatial profile is Gaussian with radius r_0.

According to assumptions *(a)* and *(b)* we shall assume the initial conditions

$$f(t, \boldsymbol{x}) = f_0^\delta(t) e^{-ik_0 t} \exp\Big(-\frac{|\boldsymbol{x}|^2}{2r_0^2}\Big), \qquad f_0^\delta(t) = \delta f_0\left(\delta t\right), \tag{38}$$

with $\delta \ll 1$ (suppressing the complex conjugate part here and below).

We next assume that

(c) the random fluctuations are statistically isotropic with correlation length l and $l \ll r_0$, moreover, $k_0 r_0 l \sim L$.

The last condition ensures that diffractive effects are of order one over a propagation distance of order L. We remark that in the random medium case diffractive effects are of order one when $k_0 r_0 l \sim L$. This is when the Rayleigh length associated with the Fresnel length, $\sqrt{r_0 l}$, is of order the depth of the slab. Note that in this configuration the random medium fluctuations give an earlier onset of diffractive effects than in the homogeneous case when the Rayleigh length associated with r_0, of order $k_0 r_0^2$, is of order the depth of the slab.

We let C_0 and D_0 represent non-dimensionalized quantities so that

$$C(z, \boldsymbol{x}) = \sigma^2 C_0\Big(\frac{z}{l}, \frac{\boldsymbol{x}}{l}\Big), \qquad D(\boldsymbol{x}) = \sigma^2 l D_0\Big(\frac{\boldsymbol{x}}{l}\Big).$$

We next assume smooth random medium fluctuations so that the autocorrelation function satisfies:

(d) $D_0(\boldsymbol{x})$ is at least twice differentiable at $\boldsymbol{x} = \mathbf{0}$.

We write

$$D(\boldsymbol{x}) = D(\mathbf{0}) - \frac{\gamma}{2}|\boldsymbol{x}|^2 + o(|\boldsymbol{x}|^2), \qquad \gamma = -\frac{1}{d}\Delta D(\mathbf{0}) = \frac{\sigma^2}{l}\gamma_0, \tag{39}$$

with $\gamma_0 = -\Delta D_0(\mathbf{0})/d$. We introduce the parameter β characterizing the strength of the forward scattering

$$\beta(k_0, L) = L\frac{\sigma^2 k_0^2 l}{4}. \tag{40}$$

Note that β corresponds to total scattering cross-section and $\beta \hat{D}_0(\cdot)$ a differential scattering cross-section, see (B3) and the discussion below. We shall then assume a relatively strong medium interaction:

(e) $\beta(k_0, L) \gg 1$.

We remark that this corresponds to $k_0^2 D(\mathbf{0}) L \gg 1$.

The other important parameter that characterizes the microstructure is $\alpha(k_0, L) = L/(k_0 l^2)$. This parameter scales the strength of the diffraction at the scale l of the random fluctuations, see (B3). Note that then assumption *(c)* implies and is in fact equivalent to

$$\alpha_0 = \frac{L}{k_0 r_0^2} \ll \alpha_e = \frac{L}{k_0 l r_0} = \mathcal{O}(1) \ll \alpha = \alpha(k_0, L) = \frac{L}{k_0 l^2}.$$

The parameters α_0, α_e and α are inverse Fresnel numbers with the aperture corresponding respectively to the source aperture r_0, random medium effective aperture $\sqrt{l r_0}$ and the medium correlation length l. They describe strength of diffractive effects for respectively homogeneous medium with source aperture r_0, the random medium with again source aperture r_0 and the homogeneous medium with source aperture l.

7.1. *Coherent Field*

Under *(a,b)* the limit of the coherent (or mean) reflected field defined by

$$v_{\rm coh,1}(t, \boldsymbol{x}) = \lim_{\varepsilon \to 0} \mathrm{E}\big[v_1^\varepsilon(t, \boldsymbol{x})\big]$$

is given by

$$\begin{aligned} v_{\rm coh,1}(t, \boldsymbol{x}) = & -\mathcal{R}_0 e^{-ik_0 t} f_0^\delta(t) e^{ik_0 \boldsymbol{\theta}\cdot\boldsymbol{x}} e^{-\frac{k_0^2}{2} D(\boldsymbol{0}) L} \\ & \times \int \psi_{\rm coh}(0, \boldsymbol{x} - \boldsymbol{x}') e^{ik\boldsymbol{\theta}\cdot\boldsymbol{x}'} \exp\Big(- \frac{|\boldsymbol{x}'|^2}{2r_0^2}\Big) d\boldsymbol{x}'. \end{aligned}$$

where $\psi_{\rm coh}(z, \boldsymbol{x})$ is the solution of the Schrödinger equation with damping

$$\frac{\partial \psi_{\rm coh}}{\partial z} = \frac{i}{k_0} \Delta_{\boldsymbol{x}} \psi_{\rm coh} - \frac{k_0^2}{4} D(\mathbf{x}) \psi_{\rm coh}$$

starting from $\psi_{\rm coh}(-L, \boldsymbol{x}) = \delta(\boldsymbol{x})$. Under *(a-c)*,

$$\psi_{\rm coh}(0, \boldsymbol{x}) = \Big(\frac{k_0}{4\pi L}\Big)^{d/2} e^{-i\frac{\pi d}{4}} \exp\Big(- i \frac{k_0 |\boldsymbol{x}|^2}{4L}\Big),$$

and therefore

$$|v_{\rm coh,1}(t, \boldsymbol{x})|^2 = \mathcal{R}_0^2 e^{-k_0^2 D(\boldsymbol{0}) L} |f_0^\delta(t)|^2 \Big(1 + \frac{4L^2}{k_0^2 r_0^4}\Big)^{-d} \exp\Big(- \frac{|\boldsymbol{x} + 2\boldsymbol{\theta} L|^2}{r_0^2 \big(1 + \frac{4L^2}{k_0^2 r_0^4}\big)}\Big). \quad (41)$$

This is the form (37) of the reflected field in the homogeneous case with an exponential damping. If moreover, random scattering is strong, assumption *(e)*, then the coherent field is vanishing.

7.2. *Incoherent Field*

Under *(a-c)*, the coherence function of the reflected field defined by

$$A_1(s,t,\boldsymbol{x},\boldsymbol{y}) = \lim_{\varepsilon\to 0} \mathrm{E}\left[v_1^\varepsilon\Big(s+\frac{t}{2},\boldsymbol{x}+\frac{\boldsymbol{y}}{2}\Big)\overline{v_1^\varepsilon}\Big(s-\frac{t}{2},\boldsymbol{x}-\frac{\boldsymbol{y}}{2}\Big)\right] \tag{42}$$

has the form

$$\begin{aligned} A_1(s,t,\boldsymbol{x},\boldsymbol{y}) &= \mathcal{R}_0^2 f_0^\delta\Big(s+\frac{t}{2}\Big)\overline{f_0^\delta}\Big(s-\frac{t}{2}\Big)e^{-ik_0t}e^{2ik_0\boldsymbol{\theta}\cdot\boldsymbol{y}} \\ &\times\Big(\frac{r_0}{2\sqrt{\pi}}\Big)^d \int e^{-\frac{r_0^2|\boldsymbol{\eta}|^2}{4}-\frac{|\boldsymbol{y}|^2}{4r_0^2}} e^{-i\boldsymbol{\eta}\cdot\boldsymbol{x}-2iL\boldsymbol{\theta}\cdot\boldsymbol{\eta}} e^{\frac{k_0^2}{4}\int_0^{2L} D(\boldsymbol{\eta}\frac{z}{k_0}+\boldsymbol{y})-D(\boldsymbol{0})dz} d\boldsymbol{\eta}. \end{aligned} \tag{43}$$

We give the details of the derivation of this result in Appendix A.

If moreover, random scattering is strong, assumption *(e)*, and the random medium fluctuations are smooth, assumption *(d)*, then we obtain that the coherence function has the Gaussian shape

$$\begin{aligned} A_1(s,t,\boldsymbol{x},\boldsymbol{y}) &= \mathcal{R}_0^2 f_0^\delta\Big(s+\frac{t}{2}\Big)\overline{f_0^\delta}\Big(s-\frac{t}{2}\Big)e^{-ik_0t}\Big(\frac{r_0}{r_R(L)}\Big)^d \\ &\times\exp\Big(-\frac{|\boldsymbol{x}+2\boldsymbol{\theta}L|^2}{r_R(L)^2}-\frac{|\boldsymbol{y}|^2}{4\rho_R(L)^2}+i\frac{(\boldsymbol{x}+2\boldsymbol{\theta}L)\cdot\boldsymbol{y}}{\chi_R(L)^2}+i2k_0\boldsymbol{\theta}\cdot\boldsymbol{y}\Big). \end{aligned} \tag{44}$$

The beam radius $r_R(L)$, the correlation radius $\rho_R(L)$, and the parameter $\chi_R(L)$ are characterized by

$$r_R(L) = r_0\sqrt{1+\frac{4\gamma L^3}{3r_0^2}}, \tag{45}$$

$$\rho_R(L) = r_0\frac{\sqrt{1+\frac{4\gamma L^3}{3r_0^2}}}{\sqrt{1+k_0^2r_0^2\gamma L+\frac{k_0^2\gamma^2L^4}{3}}}, \tag{46}$$

$$\chi_R(L) = \frac{r_R(L)}{\sqrt{k_0\gamma L^2}}, \tag{47}$$

where we have taken into account that $k_0r_0^2 \gg L$ in the considered regime.

Note that we can write respectively

$$\frac{\gamma L^3}{4r_0^2} = \gamma_0\alpha_e\beta, \qquad \frac{4\gamma L^3}{r_0^2}\frac{1}{k_0^2\gamma^2L^4} = \frac{1}{\gamma_0}\frac{(l/r_0)^2}{\beta}, \qquad \frac{\gamma L^3}{r_0^2}\frac{1}{k_0\gamma L^2} = \alpha_0,$$

so that in our scaling regime

$$\frac{r_R(L)}{r_0} \gg 1, \qquad \frac{\rho_R(L)}{r_0} \ll 1, \qquad \frac{\chi_R(L)}{r_0} \ll 1,$$

respectively. In the regime that we consider it is not possible to observe in the spatial coherence function (42) any coherent effect building up between the forward and backward propagations. In fact, one can check that the expression for the beam radius r_R and correlation radius ρ_R coincide to leading order to the ones that we would have obtained by considering propagation through independent random medium realizations in the transmission and reflection directions of propagation [6]. However, there is a very interesting coherence phenomenon that can be observed in a small angular cone and we discuss the so-called enhanced backscattering phenomenon in the next section.

8. Enhanced Backscattering

In this section, we would like to show that the reflected intensity exhibits a singular picture in a very narrow cone, of angular width of order α^{-1}, around the backscattered direction. This phenomenon called enhanced backscattering or weak localization is widely discussed in the physical literature [2, 9] and it has been observed in several experimental contexts [8, 10–12]. We remark that we here consider enhanced backscattering as associated with random medium rather than a rough surface as discussed in for instance in [7]. Enhanced backscattering refers to the situation that if a quasi-monochromatic quasi-plane wave is incoming with a given incidence angle, then the mean reflected power has a local maximum in the backscattered direction, which is twice as large as the mean reflected power in the other directions. In this section, we give a mathematical proof of enhanced backscattering and we deduce the maximum, the angular width, and the shape of the enhanced backscattering cone.

8.1. *Enhanced Backscattering from a Strong Interface*

In this section, we assume that the incoming wave has the form

$$f(t,\boldsymbol{x}) = f_0^\delta(t)e^{-ik_0t}g_{\rm inc}(\boldsymbol{x}),$$

that it is narrowband as above, and that it is nearly a plane wave, in the sense that $\hat{g}_{\rm inc}(\boldsymbol{\kappa})$ is concentrated at some $\boldsymbol{\kappa}_{\rm inc}$ (assumed to be different from the vector $\boldsymbol{\theta}$ corresponding to normal incidence on the interface). By "concentrated" we mean that the angular width of the incoming beam is smaller than α^{-1}. The first reflected signal in the direction $\boldsymbol{\kappa}_0$ is

$$\widetilde{v}_1^\varepsilon(s,\boldsymbol{\kappa}_0) = \int v_1^\varepsilon(s,\boldsymbol{x})e^{-i\boldsymbol{\kappa}_0\cdot\boldsymbol{x}}d\boldsymbol{x}.$$

From (26-28-27) we have

$$\widetilde{v}_1^\varepsilon(s,\boldsymbol{\kappa}_0) = -\frac{1}{2\pi}\iint \widetilde{\boldsymbol{\mathcal{R}}}^\varepsilon(k+k_0,0,\boldsymbol{x},\boldsymbol{x}')e^{i(k+k_0)(\boldsymbol{\theta}\cdot\boldsymbol{x}+\boldsymbol{\theta}\cdot\boldsymbol{x}')}\hat{f}\left(\frac{k}{\delta}\right)g_{\rm inc}(\boldsymbol{x}')d\boldsymbol{x}'$$
$$\times\, e^{-i(k+k_0)s}dke^{-i\boldsymbol{\kappa}_0\cdot\boldsymbol{x}}d\boldsymbol{x}.$$

We then find

$$\widetilde{v}_1^\varepsilon(s,\boldsymbol{\kappa}_0) = -\frac{1}{2\pi}\iint \widehat{\boldsymbol{\mathcal{R}}}^\varepsilon(k+k_0,0,\boldsymbol{\kappa}_0-(k+k_0)\boldsymbol{\theta},\boldsymbol{\kappa}'+(k+k_0)\boldsymbol{\theta})\hat{f}\left(\frac{k}{\delta}\right)\hat{g}_{\rm inc}(\boldsymbol{\kappa}')$$
$$\times\, e^{-i(k+k_0)s}dkd\boldsymbol{\kappa}'. \tag{48}$$

The mean of the square modulus of $\widetilde{v}_1^\varepsilon(s,\boldsymbol{\kappa}_0)$ only involves the mean of the product of a pair of reflection kernels, and it follows that this mean converges to the mean of the square modulus of the limit process $\widetilde{v}_1(s, \boldsymbol{\kappa}_0)$ defined as the Fourier transform in $\boldsymbol{x}$ of $v_1(s, \boldsymbol{x})$ given by (30) [6]. This means that the mean reflected intensity in the direction $\boldsymbol{\kappa}_0$ satisfies

$$\lim_{\varepsilon \to 0} \mathrm{E}\left[|\widetilde{v}_1^\varepsilon(s, \boldsymbol{\kappa}_0)|^2\right] = \mathcal{R}_0^2 |f_0^\delta(s)|^2 I^R(\boldsymbol{\kappa}_0), \tag{49}$$
$$I^R(\boldsymbol{\kappa}_0) = 2^{-d} l_x^d \int \mathcal{V}^R\Big(1, \frac{\boldsymbol{\kappa}_0 - \boldsymbol{\kappa}_1' - 2k_0\boldsymbol{\theta}}{2} l, (\boldsymbol{\kappa}_0 + \boldsymbol{\kappa}_1')l, \mathbf{0}\Big) |\hat{g}_{\mathrm{inc}}(\boldsymbol{\kappa}_1')|^2 d\boldsymbol{\kappa}_1'.$$

Here $\mathcal{V}^R$ is a transformed Wigner transform and is introduced in Appendix B. We derive this result in Appendix C. Using the fact that $\hat{g}_{\mathrm{inc}}(\boldsymbol{\kappa})$ is concentrated at $\boldsymbol{\kappa}_{\mathrm{inc}}$, we get

$$I^R(\boldsymbol{\kappa}_0) \simeq P_{\mathrm{inc}} \mathcal{V}^R\Big(1, \frac{\boldsymbol{\kappa}_0 - (\boldsymbol{\kappa}_{\mathrm{inc}} + 2k_0\boldsymbol{\theta})}{2} l, (\boldsymbol{\kappa}_0 + \boldsymbol{\kappa}_{\mathrm{inc}})l, \mathbf{0}\Big), \tag{50}$$

where $P_{\mathrm{inc}} = 2^{-d} l_x^d \int |\hat{g}_{\mathrm{inc}}(\boldsymbol{\kappa}_1')|^2 d\boldsymbol{\kappa}_1'$. This formula gives the mean reflected intensity in the direction $\boldsymbol{\kappa}_0$ and is valid for arbitrary values of α and β. Let us consider the regime $\alpha \gg 1$. The mean reflected intensity far enough from the backscattered direction $-\boldsymbol{\kappa}_{\mathrm{inc}}$ is of the form

$$\begin{aligned} I^R(\boldsymbol{\kappa}_0) &= P_{\mathrm{inc}} \mathcal{V}_{\mathbf{0}}^R\Big(1, \frac{\boldsymbol{\kappa}_0 - (\boldsymbol{\kappa}_{\mathrm{inc}} + 2k_0\boldsymbol{\theta})}{2} l\Big) \\ &= \frac{P_{\mathrm{inc}}}{(2\pi)^d} \int e^{-il(\boldsymbol{\kappa}_0 - (\boldsymbol{\kappa}_{\mathrm{inc}} + 2k_0\boldsymbol{\theta}))\cdot \boldsymbol{u}/2} e^{2\beta(D_0(\frac{\boldsymbol{u}}{2}) - D_0(\mathbf{0}))} d\boldsymbol{u}, \end{aligned} \tag{51}$$

for $|\boldsymbol{\kappa}_0 + \boldsymbol{\kappa}_{\mathrm{inc}}| l \gg \alpha^{-1}$, where we have used the second point of Lemma B.1. In a narrow angular cone around the backscattered direction $-\boldsymbol{\kappa}_{\mathrm{inc}}$, the reflected intensity is locally larger:

$$\begin{aligned} I^R(-\boldsymbol{\kappa}_{\mathrm{inc}} + \alpha^{-1}\boldsymbol{\kappa}) &= P_{\mathrm{inc}}\left[\mathcal{V}_{\mathbf{0}}^R(1, -(\boldsymbol{\kappa}_{\mathrm{inc}} + k_0\boldsymbol{\theta})l) + \mathcal{V}_{\boldsymbol{\kappa}l}^R(1, -(\boldsymbol{\kappa}_{\mathrm{inc}} + k_0\boldsymbol{\theta})l)\right] \\ &= \frac{P_{\mathrm{inc}}}{(2\pi)^d}\Big[\int e^{il(\boldsymbol{\kappa}_{\mathrm{inc}} + k_0\boldsymbol{\theta})\cdot\boldsymbol{u}} e^{2\beta(D_0(\frac{\boldsymbol{u}}{2}) - D_0(\mathbf{0}))} d\boldsymbol{u} \\ &\quad + \int e^{il(\boldsymbol{\kappa}_{\mathrm{inc}} + k_0\boldsymbol{\theta})\cdot\boldsymbol{u}} e^{\beta\int_{-1}^1 D_0(\frac{\boldsymbol{u}}{2} + \boldsymbol{\kappa}l\zeta') - D_0(\mathbf{0}) d\zeta'} d\boldsymbol{u}\Big], \end{aligned} \tag{52}$$

where we have used the third point of Lemma B.1. Note that in the regime of $\beta \ll 1$ we see from (51) that we have sharp specular reflection in the direction $\boldsymbol{\kappa}_{\mathrm{inc}} + 2k_0\boldsymbol{\theta}$ and from (52) that the enhanced backscattering cone vanishes in this limit. If we assume that $\beta \gg 1$, then the main contribution to the integral in (51) is concentrated to small $|\boldsymbol{u}|$ and we can replace

$$e^{2\beta(D_0(\frac{\boldsymbol{u}}{2}) - D_0(\mathbf{0}))} \approx e^{\beta \Delta D_0(\mathbf{0})|\boldsymbol{u}|^2/(4d)} = e^{-\beta\gamma_0|\boldsymbol{u}|^2/4},$$

so that

$$I^R(\boldsymbol{\kappa}_0) = P_{\mathrm{inc}}(\pi\gamma_0\beta)^{-d/2} \exp\Big(-\frac{|\boldsymbol{\kappa}_0 - (\boldsymbol{\kappa}_{\mathrm{inc}} + 2k_0\boldsymbol{\theta})|^2 l^2}{4\gamma_0\beta}\Big), \tag{53}$$

for $|\boldsymbol{\kappa}_0 + \boldsymbol{\kappa}_{\mathrm{inc}}| l \gg \alpha^{-1}$, where γ_0 is the dimensionless version of γ given by (39): $\gamma = \sigma^2 l^{-1}\gamma_0$. This formula gives the width of the diffusive cone around the "specular direction" $\boldsymbol{\kappa}_{\rm inc} + 2k_0\boldsymbol{\theta}$:

$$\Delta\kappa_{\rm spec} = \frac{2\sqrt{\gamma_0\beta}}{l} = \sqrt{\gamma L}k_0 = \frac{2}{\rho_R(L)}. \tag{54}$$

Thus, we see that a rapid decorrelation of the reflected field corresponds to a diffuse and broad specular cone.

On the top of this broad cone, we have a narrow cone of relative maximum equal to 2 centered along the backscattered direction $-\boldsymbol{\kappa}_{\rm inc}$:

$$\begin{aligned} I^R(-\boldsymbol{\kappa}_{\rm inc} + \alpha^{-1}\boldsymbol{\kappa}) = P_{\rm inc}(\pi\gamma_0\beta)^{-d/2} \exp\Big(- \frac{|\boldsymbol{\kappa}_{\rm inc} + k_0\boldsymbol{\theta}|^2 l^2}{\gamma_0\beta}\Big) \\ \times \Big[1 + \exp\Big(- \frac{\gamma_0\beta}{3}|\boldsymbol{\kappa}|^2 l^2\Big)\Big]. \end{aligned} \tag{55}$$

This shows then that the width of the enhanced backscattering cone is

$$\Delta\kappa_{\rm EBC} = \frac{\sqrt{3}}{l\sqrt{\gamma_0\beta}\alpha} = \frac{2\sqrt{3}}{\sqrt{\gamma L^3}} = \frac{4}{r_R(L)}. \tag{56}$$

Therefore, a wide broadening of the reflected wave energy goes with a relatively sharp enhanced backscattering cone. We remark that the results (53) and (55) are based on the assumption of a smooth correlation function, assumption (d), and indeed then the shapes of the specular and backscattering cones are smooth in general and Gaussian when $\beta \gg 1$. In the case when the backscattering comes from the medium fluctuations only, then the shapes of the specular and backscattering cones depend sensitively on the roughness of the medium. In particular the backscattering cone can have a cusp for rough media [5]. Note that the angular width of the backscattering cone is thus

$$\Delta\theta_{\rm EBC} = \frac{\Delta\kappa_{\rm EBC}}{k_0} = \frac{4}{k_0 r_R(L)} \tag{57}$$

is proportional to the wavelength, as predicted by physical arguments based on diagrammatic expansions [9]. The reciprocal relation to the beam spreading is also in agreement with the physical interpretation of enhanced backscattering as a constructive interference between pairs of wave "paths" and reversed paths (see Figure 2). The sum of all these constructive interferences should give an enhancement factor of 2 in the backscattered direction as follows from the following heuristic argument. Assume that the reflected wave is observed with an angle A. For paths corresponding to $A = 0$ there are two perfectly correlated paths, while for A large they become independent. The factor of two then corresponds to the variance of two perfectly correlated random variables relative to the variance when they are independent. Note that the cone of correlated directions then will give the width of the enhanced backscattering cone. Now, if the reflected wave is observed with an angle A compared to the backscattered direction, then the phase shift between the direct and reversed paths is $ke = kd\sin A$, where d is the typical transverse size of a wave path, which is in our setting of the order of the beam width r_R. Therefore, constructive interference is possible in the approximate range $k_0 r_R A \leq \pi$, which gives the angular aperture of the enhanced backscattering cone. This "path" interpretation is not used in our paper, but we recover the physical result by exploiting our Itô-Schrödinger model.

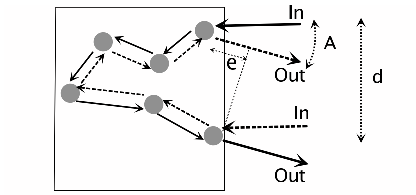

Figure 2. Physical interpretation of the scattering of a plane wave by a random medium. The output wave in direction A is the superposition of many different scattering paths. One of these paths is plotted as well as the reversed path. The phase difference between the two outgoing waves is $ke = kd \sin A$.

8.2. *Enhanced Backscattering from a Diffusive Interface*

We discuss in this section the enhanced backscattering cone in the case of a diffusive interface and show that indeed it is robust with respect such a model generalization. In the previous sections we considered the case of a specular reflection at the interface. For applications, it is important to discuss the case of diffusive backscattering. In this subsection, we revisit the theory in the case in which an inhomogeneous interface is inserted in the plane $z = -L - \varepsilon^2 \boldsymbol{\theta} \cdot \boldsymbol{x}$, with the impedance $Z_M(\boldsymbol{x}/\varepsilon^2)$, so that the second boundary condition (11) now reads

$$\widetilde{a}^\varepsilon(k, -L, \boldsymbol{x}) e^{-ik\frac{L}{\varepsilon^4}} - R_M(\boldsymbol{x}) \widetilde{b}^\varepsilon(k, -L, \boldsymbol{x}) e^{ik\frac{L}{\varepsilon^4}} = 0,$$

where $R_M(\boldsymbol{x}) = (Z_M(\boldsymbol{x}) - 1)/(Z_M(\boldsymbol{x}) + 1)$ is the local reflection coefficient of the interface. In this case, the initial condition at $z = -L$ for the reflection operator is

$$\widetilde{\boldsymbol{\mathcal{R}}}^\varepsilon(k, -L, \boldsymbol{x}, \boldsymbol{x}') = R_M(\boldsymbol{x}) \delta(\boldsymbol{x} - \boldsymbol{x}').$$

We shall assume here that R_M is a stationary random process, with mean zero and autocorrelation function

$$\mathrm{E}[R_M(\boldsymbol{x}) \overline{R_M}(\boldsymbol{x}')] = R_0^2 \psi(\boldsymbol{x} - \boldsymbol{x}').$$

We can repeat the arguments of Appendix C and find that the reflected intensity is still given by (50). In fact the only change is in the initial condition for the transformed Wigner transform $\mathcal{V}^R$. The enhanced backscattering cone can then be found by an argument as in the previous section, using the results of Lemma B.2 rather than Lemma B.1.

Now the mean reflected intensity far enough from the backscattered direction $-\boldsymbol{\kappa}_{\rm inc}$ is of the form

$$I^R(\boldsymbol{\kappa}_0) = \frac{P_{\rm inc}}{(2\pi)^d} \int \psi\left(\frac{l\boldsymbol{u}}{2}\right) e^{-il(\boldsymbol{\kappa}_0 - (\boldsymbol{\kappa}_{\rm inc} + 2k_0\boldsymbol{\theta}) \cdot \boldsymbol{u}/2} e^{2\beta(D_0(\frac{\boldsymbol{u}}{2}) - D_0(\boldsymbol{0}))} d\boldsymbol{u}, \quad (58)$$

for $|\boldsymbol{\kappa}_0 + \boldsymbol{\kappa}_{\rm inc}| l \gg \alpha^{-1}$, where we have used the second point of Lemma B.2. To get simple explicit expressions for the characteristics of the reflected wave we assume that ψ is Gaussian:

$$\psi(\boldsymbol{x}) = e^{-\frac{|\boldsymbol{x}|^2}{a^2}}, \quad (59)$$

where a is the correlation radius of the diffusive interface. We then find when $\beta \gg 1$ that

$$I^R(\boldsymbol{\kappa}_0) = P_{\rm inc}(\pi(\gamma_0\beta + (l/a)^2)^{-d/2} \exp\Big(-\frac{|\boldsymbol{\kappa}_0 - (\boldsymbol{\kappa}_{\rm inc} + 2k_0\boldsymbol{\theta})|^2 l^2}{4(\gamma_0\beta + (l/a)^2)}\Big), \quad (60)$$

for $|\boldsymbol{\kappa}_0 + \boldsymbol{\kappa}_{\rm inc}| l \gg \alpha^{-1}$. This formula gives the width of the diffusive cone around the "specular direction" $\boldsymbol{\kappa}_{\rm inc} + 2k_0\boldsymbol{\theta}$:

$$\Delta\kappa^a_{\rm spec} = \frac{2\sqrt{\gamma_0\beta + (l/a)^2}}{l} = k_0\sqrt{\gamma L + 4/(ak_0)^2}. \tag{61}$$

which shows that the diffusive interface broadens the specular cone and the angular broadening becomes strong when $k_0 a \ll 1$. Correspondingly, in a narrow angular cone around the backscattered direction $-\boldsymbol{\kappa}_{\rm inc}$, the reflected intensity is locally larger, now given by:

$$\begin{aligned} I^R(-\boldsymbol{\kappa}_{\rm inc} + \alpha^{-1}\boldsymbol{\kappa}) = \frac{P_{\rm inc}}{(2\pi)^d}\Big[\int \psi\left(\frac{l\boldsymbol{u}}{2}\right) e^{il(\boldsymbol{\kappa}_{\rm inc}+k_0\boldsymbol{\theta})\cdot\boldsymbol{u}} e^{2\beta(D_0(\frac{\boldsymbol{u}}{2})-D_0(\boldsymbol{0}))} d\boldsymbol{u} \\ + \int \psi\left(\frac{l\boldsymbol{u}}{2}\right) e^{il(\boldsymbol{\kappa}_{\rm inc}+k_0\boldsymbol{\theta})\cdot\boldsymbol{u}} e^{\beta\int_{-1}^1 D_0(\frac{\boldsymbol{u}}{2}+\boldsymbol{\kappa}l\zeta')-D_0(\boldsymbol{0})d\zeta'} d\boldsymbol{u}\Big], \end{aligned}$$

where we have used the third point of Lemma B.2. It then again follows that, when $\beta \gg 1$, on the top of the broad cone, we have a narrow cone of relative maximum equal to 2 centered along the backscattered direction $-\boldsymbol{\kappa}_{\rm inc}$:

$$\begin{aligned} I^R(-\boldsymbol{\kappa}_{\rm inc} + \alpha^{-1}\boldsymbol{\kappa}) = P_{\rm inc}(\pi(\gamma_0\beta + (l/a)^2)^{-d/2} \exp\Big(- \frac{|\boldsymbol{\kappa}_{\rm inc} + k_0\boldsymbol{\theta}|^2 l^2}{\gamma_0\beta + (l/a)^2}\Big) \\ \times \Big[1 + \exp\Big(- \frac{\gamma_0\beta}{3}|\boldsymbol{\kappa}|^2 l^2\Big)\Big]. \end{aligned} \tag{62}$$

Observe that relative magnitude and width of the cone are not affected by the replacement of the specular interface with a diffusive interface.

Appendix A. Coherence Function of the Reflected Wave

We derive the expression (43) for the form of the coherence function of the reflected wave defined by (42). We find using (30) that

$$\begin{aligned} A_1(s,t,\boldsymbol{x},\boldsymbol{y}) = \frac{1}{(2\pi)^2}\iint {\rm E}\Big[\widetilde{\boldsymbol{\mathcal{R}}}(k,0,\boldsymbol{x}+\frac{\boldsymbol{y}}{2},\boldsymbol{x}')\overline{\widetilde{\boldsymbol{\mathcal{R}}}(k,0,\boldsymbol{x}-\frac{\boldsymbol{y}}{2},\boldsymbol{x}'')}\Big] \\ \times e^{ik\boldsymbol{\theta}\cdot(\boldsymbol{x}+\frac{\boldsymbol{y}}{2}+\boldsymbol{x}')}\widetilde{f^\delta}(k,\boldsymbol{x}')d\boldsymbol{x}'e^{-ik(s+\frac{t}{2})}dk e^{-ik'\boldsymbol{\theta}\cdot(\boldsymbol{x}-\frac{\boldsymbol{y}}{2}+\boldsymbol{x}'')}\overline{\widetilde{f^\delta}(k',\boldsymbol{x}'')}d\boldsymbol{x}''e^{-ik'(s-\frac{t}{2})}dk'. \end{aligned}$$

Note that

$$\widetilde{f^\delta}(k,\boldsymbol{x}) = e^{-\frac{|\boldsymbol{x}|^2}{2r_0^2}}\hat{f}\Big(\frac{k-k_0}{\delta}\Big).$$

In view of the narrow bandwidth assumption we then get

$$
\begin{aligned}
A_1(s,t,\boldsymbol{x},\boldsymbol{y}) &= \frac{1}{(2\pi)^2}\iint \mathrm{E}\left[\widetilde{\boldsymbol{\mathcal{R}}}(k_0,0,\boldsymbol{x}+\frac{\boldsymbol{y}}{2},\boldsymbol{x}')\overline{\widetilde{\boldsymbol{\mathcal{R}}}(k_0,0,\boldsymbol{x}-\frac{\boldsymbol{y}}{2},\boldsymbol{x}'')}\right] e^{-\frac{|\boldsymbol{x}'|^2}{2r_0^2}} e^{-\frac{|\boldsymbol{x}''|^2}{2r_0^2}} \\
&\times \hat{f}\left(\frac{k}{\delta}\right)\overline{\hat{f}}\left(\frac{k'}{\delta}\right) e^{ik_0\boldsymbol{\theta}\cdot(\boldsymbol{x}'-\boldsymbol{x}''+\boldsymbol{y}-t)} e^{-i(k+k')t/2} e^{-i(k-k')s} dk dk' d\boldsymbol{x}' d\boldsymbol{x}'' \\
&= \iint \mathrm{E}\left[\widetilde{\boldsymbol{\mathcal{R}}}(k_0,0,\boldsymbol{x}+\frac{\boldsymbol{y}}{2},\boldsymbol{x}')\overline{\widetilde{\boldsymbol{\mathcal{R}}}(k_0,0,\boldsymbol{x}-\frac{\boldsymbol{y}}{2},\boldsymbol{x}'')}\right] e^{-\frac{|\boldsymbol{x}'|^2+|\boldsymbol{x}''|^2}{2r_0^2}} \\
&\times f_0^\delta(s+t/2)\overline{f_0^\delta(s-t/2)} e^{ik_0(\boldsymbol{\theta}\cdot(\boldsymbol{x}'-\boldsymbol{x}''+\boldsymbol{y})-t)} d\boldsymbol{x}' d\boldsymbol{x}''.
\end{aligned}
$$

In order to characterize the coherence function A_1 we introduce the Wigner transform of the reflection operator defined by

$$
\begin{aligned}
W_k^{\mathrm{R}}(z,\boldsymbol{x},\boldsymbol{x}',\boldsymbol{\kappa},\boldsymbol{\kappa}') &= \iint e^{-i(\boldsymbol{\kappa}\cdot\boldsymbol{y}+\boldsymbol{\kappa}'\cdot\boldsymbol{y}')} \\
&\times \mathrm{E}\Big[\widetilde{\boldsymbol{\mathcal{R}}}\Big(k,-z,\boldsymbol{x}+\frac{\boldsymbol{y}}{2},\boldsymbol{x}'+\frac{\boldsymbol{y}'}{2}\Big)\overline{\widetilde{\boldsymbol{\mathcal{R}}}\Big(k,-z,\boldsymbol{x}-\frac{\boldsymbol{y}}{2},\boldsymbol{x}'-\frac{\boldsymbol{y}'}{2}\Big)}\Big] d\boldsymbol{y} d\boldsymbol{y}' .
\end{aligned} \tag{A1}
$$

It satisfies a set of transport equations:

$$
\begin{aligned}
\frac{\partial W_k^{\mathrm{R}}}{\partial z} + \frac{\boldsymbol{\kappa}}{k}\cdot\nabla_{\boldsymbol{x}} W_k^{\mathrm{R}} + \frac{\boldsymbol{\kappa}'}{k}\cdot\nabla_{\boldsymbol{x}'} W_k^{\mathrm{R}} &= \frac{k^2}{4(2\pi)^d}\int \hat{D}(\boldsymbol{u}) \\
\times\Big[W_k^{\mathrm{R}}\big(z,\boldsymbol{x},\boldsymbol{x}',\boldsymbol{\kappa}-\boldsymbol{u},\boldsymbol{\kappa}'\big) &+ W_k^{\mathrm{R}}\big(z,\boldsymbol{x},\boldsymbol{x}',\boldsymbol{\kappa},\boldsymbol{\kappa}'-\boldsymbol{u}\big) \\
&+2W_k^{\mathrm{R}}\Big(z,\boldsymbol{x},\boldsymbol{x}',\boldsymbol{\kappa}-\frac{1}{2}\boldsymbol{u},\boldsymbol{\kappa}'-\frac{1}{2}\boldsymbol{u}\Big)\cos\big(\boldsymbol{u}\cdot(\boldsymbol{x}-\boldsymbol{x}')\big) \\
&-2W_k^{\mathrm{R}}\Big(z,\boldsymbol{x},\boldsymbol{x}',\boldsymbol{\kappa}-\frac{1}{2}\boldsymbol{u},\boldsymbol{\kappa}'+\frac{1}{2}\boldsymbol{u}\Big)\cos\big(\boldsymbol{u}\cdot(\boldsymbol{x}-\boldsymbol{x}')\big) \\
&-2W_k^{\mathrm{R}}\big(z,\boldsymbol{x},\boldsymbol{x}',\boldsymbol{\kappa},\boldsymbol{\kappa}'\big)\Big] d\boldsymbol{u},
\end{aligned} \tag{A2}
$$

starting from $W_k^{\mathrm{R}}(z=L,\boldsymbol{x},\boldsymbol{x}',\boldsymbol{\kappa},\boldsymbol{\kappa}') = (2\pi)^d\mathcal{R}_0^2\delta(\boldsymbol{x}-\boldsymbol{x}')\delta(\boldsymbol{\kappa}+\boldsymbol{\kappa}')$. The coherence function can now be expressed as

$$
\begin{aligned}
A_1(s,t,\boldsymbol{x},\boldsymbol{y}) &= \mathcal{H}(\boldsymbol{x},\boldsymbol{y})\mathcal{R}_0^2 f_0^\delta(s+t/2)\overline{f_0^\delta(s-t/2)} e^{ik_0(\boldsymbol{\theta}\cdot\boldsymbol{y}-t)}, \\
\mathcal{H}(\boldsymbol{x},\boldsymbol{y}) &= \frac{1}{(2\pi)^{2d}\mathcal{R}_0^2}\iint W_{k_0}^{\mathrm{R}}(0,\boldsymbol{x},\frac{\boldsymbol{x}'+\boldsymbol{x}''}{2},\boldsymbol{\kappa},\boldsymbol{\kappa}') e^{i(\boldsymbol{\kappa}\cdot\boldsymbol{y}+\boldsymbol{\kappa}'\cdot(\boldsymbol{x}'-\boldsymbol{x}''))} d\boldsymbol{\kappa} d\boldsymbol{\kappa}' \\
&\times e^{-\frac{|\boldsymbol{x}'|^2+|\boldsymbol{x}''|^2}{2r_0^2}} e^{ik_0\boldsymbol{\theta}\cdot(\boldsymbol{x}'-\boldsymbol{x}'')} d\boldsymbol{x}' d\boldsymbol{x}''.
\end{aligned} \tag{A3}
$$

From (B1) and (B2) we have

$$
\begin{aligned}
W_k^{\mathrm{R}}(0,\boldsymbol{x},\boldsymbol{x}',\boldsymbol{\kappa},\boldsymbol{\kappa}') &= \mathcal{R}_0^2(l/2)^d\int e^{i\boldsymbol{\kappa}''\cdot(\boldsymbol{x}'-\boldsymbol{x})} e^{iz(\boldsymbol{\kappa}-\boldsymbol{\kappa}')\cdot\boldsymbol{\kappa}''/k} \\
&\times \mathcal{V}^{\mathrm{R}}\Big(1, l(\boldsymbol{\kappa}+\boldsymbol{\kappa}')/2, l(\boldsymbol{\kappa}-\boldsymbol{\kappa}'), l\boldsymbol{\kappa}''; \alpha(k_0,L),\beta(k_0,L)\Big) d\boldsymbol{\kappa}'',
\end{aligned}
$$

with $\alpha(k,z) = z/(kl^2)$ scaling the diffraction strength and $\beta(k,z) = z\sigma^2 k^2 l/4$ characterizing the strength of forward scattering. We then find

$$\mathcal{H}(\boldsymbol{x},\boldsymbol{y}) = \frac{1}{(2\pi)^{2d}}\left(\frac{l}{2}\right)^d \iint e^{i\boldsymbol{\kappa}''\cdot((\boldsymbol{x}'+\boldsymbol{x}'')/2-\boldsymbol{x})} e^{iL(\boldsymbol{\kappa}-\boldsymbol{\kappa}')\cdot\boldsymbol{\kappa}''/k_0}$$
$$\times \mathcal{V}^{\mathrm{R}}\Big(1, l(\boldsymbol{\kappa}+\boldsymbol{\kappa}')/2, l(\boldsymbol{\kappa}-\boldsymbol{\kappa}'), l\boldsymbol{\kappa}''; \alpha(k_0,L), \beta(k_0,L)\Big) d\boldsymbol{\kappa}'' e^{i(\boldsymbol{\kappa}\cdot\boldsymbol{y}+\boldsymbol{\kappa}'\cdot(\boldsymbol{x}'-\boldsymbol{x}''))} d\boldsymbol{\kappa} d\boldsymbol{\kappa}'$$
$$\times e^{-\frac{|\boldsymbol{x}'|^2+|\boldsymbol{x}''|^2}{2r_0^2}} e^{ik_0\boldsymbol{\theta}\cdot(\boldsymbol{x}'-\boldsymbol{x}'')} d\boldsymbol{x}' d\boldsymbol{x}''$$
$$= \left(\frac{1}{2(2\pi l)^2}\right)^d \iint e^{i\boldsymbol{s}\cdot((\boldsymbol{x}'+\boldsymbol{x}'')/2-\boldsymbol{x})/l} e^{iL\boldsymbol{r}\cdot\boldsymbol{s}/(k_0 l^2)}$$
$$\times \mathcal{V}^{\mathrm{R}}\Big(1, \boldsymbol{q}, \boldsymbol{r}, \boldsymbol{s}; \alpha(k_0,L), \beta(k_0,L)\Big) e^{i((\boldsymbol{q}+\boldsymbol{r}/2)\cdot\boldsymbol{y}+(\boldsymbol{q}-\boldsymbol{r}/2)\cdot(\boldsymbol{x}'-\boldsymbol{x}''))/l} d\boldsymbol{q} d\boldsymbol{r} d\boldsymbol{s}$$
$$\times e^{-\frac{|\boldsymbol{x}'|^2+|\boldsymbol{x}''|^2}{2r_0^2}} e^{ik_0\boldsymbol{\theta}\cdot(\boldsymbol{x}'-\boldsymbol{x}'')} d\boldsymbol{x}' d\boldsymbol{x}''$$

Integrating the Gaussians in $\boldsymbol{x}', \boldsymbol{x}''$ we get

$$\mathcal{H}(\boldsymbol{x},\boldsymbol{y}) = \left(\frac{r_0^2}{4\pi l^2}\right)^d \iint e^{-i\boldsymbol{s}\cdot\boldsymbol{x}/l} e^{i\alpha(k_0,L)\boldsymbol{r}\cdot\boldsymbol{s}} e^{i((\boldsymbol{q}+\boldsymbol{r}/2)\cdot\boldsymbol{y}/l}$$
$$\times \mathcal{V}^{\mathrm{R}}\Big(1, \boldsymbol{q}, \boldsymbol{r}, \boldsymbol{s}; \alpha(k_0,L), \beta(k_0,L)\Big) e^{-r_0^2(|k_0\boldsymbol{\theta}+(\boldsymbol{q}-\boldsymbol{r}/2)/l|^2+|\boldsymbol{s}/(2l)|^2)} d\boldsymbol{q} d\boldsymbol{r} d\boldsymbol{s}.$$

Next, we make the transformations $\boldsymbol{r} \mapsto \boldsymbol{r}+2\boldsymbol{q}$, $\boldsymbol{s} \mapsto \boldsymbol{s}/(2\alpha(k_0,L))$ and get

$$\mathcal{H}(\boldsymbol{x},\boldsymbol{y}) = \left(\frac{r_0^2}{8\pi l^2\alpha(k_0,L)}\right)^d \iint e^{-i\boldsymbol{s}\cdot\boldsymbol{x}/(2l\alpha(k_0,L))} e^{i(\boldsymbol{q}+\boldsymbol{r}/2)\cdot\boldsymbol{s}} e^{i((2\boldsymbol{q}+\boldsymbol{r}/2)\cdot\boldsymbol{y}/l}$$
$$\times \mathcal{V}^{\mathrm{R}}\Big(1, \boldsymbol{q}, \boldsymbol{r}+2\boldsymbol{q}, \frac{\boldsymbol{s}}{2\alpha(k_0,L)}; \alpha(k_0,L), \beta(k_0,L)\Big)$$
$$\times e^{-r_0^2(|k_0\boldsymbol{\theta}-\boldsymbol{r}/(2l)|^2+|\boldsymbol{s}/(4\alpha(k_0,L)l)|^2)} d\boldsymbol{q} d\boldsymbol{r} d\boldsymbol{s}.$$

Next we use Lemma B.1 to get

$$\mathcal{H}(\boldsymbol{x},\boldsymbol{y}) = \left(\frac{r_0^2}{16\pi^2 l^2\alpha(k_0,L)}\right)^d \iint e^{-i\boldsymbol{s}\cdot\boldsymbol{x}/(2l\alpha(k_0,L))} e^{i(\boldsymbol{r}/2+\boldsymbol{q})\cdot\boldsymbol{s}} e^{i((2\boldsymbol{q}+\boldsymbol{r}/2)\cdot\boldsymbol{y}/l}$$
$$\times e^{-i\boldsymbol{q}\cdot\boldsymbol{u}} e^{\beta(k_0,L)\int_{-1}^1 D_0(\frac{\boldsymbol{u}}{2}+\frac{\boldsymbol{s}}{2}\zeta)-D_0(\boldsymbol{0})d\zeta} e^{-r_0^2(|k_0\boldsymbol{\theta}-\boldsymbol{r}/(2l)|^2+|\boldsymbol{s}/(4\alpha(k_0,L)l)|^2)} d\boldsymbol{q} d\boldsymbol{r} d\boldsymbol{s} d\boldsymbol{u}.$$

Integrating in $\boldsymbol{q}$ and evaluating the associated Dirac delta function we get

$$\mathcal{H}(\boldsymbol{x},\boldsymbol{y}) = \left(\frac{r_0^2}{8\pi l^2\alpha(k_0,L)}\right)^d \iint e^{-i\boldsymbol{s}\cdot\boldsymbol{x}/(2l\alpha(k_0,L))} e^{i\boldsymbol{r}\cdot(\boldsymbol{s}+\boldsymbol{y}/l)/2}$$
$$\times e^{2\beta(k_0,L)\int_0^1 D_0(\frac{\boldsymbol{y}}{l}+\boldsymbol{s}\zeta)-D_0(\boldsymbol{0})d\zeta} \times e^{-r_0^2(|k_0\boldsymbol{\theta}-\boldsymbol{r}/(2l)|^2+|\boldsymbol{s}/(4\alpha(k_0,L)l)|^2)} d\boldsymbol{r} d\boldsymbol{s}.$$

Integrating in $\boldsymbol{r}$ we then get

$$\mathcal{H}(\boldsymbol{x},\boldsymbol{y}) = \left(\frac{r_0}{4\sqrt{\pi} l\alpha(k_0,L)}\right)^d \int e^{-i\boldsymbol{s}\cdot\boldsymbol{x}/(2l\alpha(k_0,L))} e^{ik_0\boldsymbol{\theta}\cdot(\boldsymbol{y}+\boldsymbol{s}l)} e^{-\frac{|\boldsymbol{y}+\boldsymbol{s}l|^2}{4r_0^2}}$$
$$\times e^{-\left|\frac{r_0\boldsymbol{s}}{4\alpha(k_0,L)l}\right|^2} e^{2\beta(k_0,L)\int_0^1 D_0(\frac{\boldsymbol{y}}{l}+\boldsymbol{s}\zeta)-D_0(\boldsymbol{0})d\zeta} d\boldsymbol{s}.$$

Using that $D(\boldsymbol{x}) = \sigma^2 l D_0(\boldsymbol{x}/l)$ we can rewrite as

$$\begin{aligned}\mathcal{H}(\boldsymbol{x},\boldsymbol{y}) &= \left(\frac{r_0}{2\sqrt{\pi}}\right)^d \int e^{-i\boldsymbol{\eta}\cdot\boldsymbol{x}} e^{ik_0\boldsymbol{\theta}\cdot(\boldsymbol{y}+2\boldsymbol{\eta}L/k_0))} e^{-\frac{|\boldsymbol{y}+2\boldsymbol{\eta}L/k_0|^2}{4r_0^2}} \\ &\qquad \times e^{-\frac{|r_0\boldsymbol{\eta}|^2}{4}} e^{\frac{k_0^2}{4}\int_0^{2L} D(\boldsymbol{y}+\frac{\boldsymbol{\eta}\zeta}{k_0})-D(\boldsymbol{0})d\zeta} d\boldsymbol{\eta} \\ &\simeq \left(\frac{r_0}{2\sqrt{\pi}}\right)^d \int e^{-i\boldsymbol{\eta}\cdot\boldsymbol{x}} e^{ik_0\boldsymbol{\theta}\cdot(\boldsymbol{y}+2\boldsymbol{\eta}L/k_0))} e^{-\frac{|\boldsymbol{y}|^2}{4r_0^2}} \\ &\qquad \times e^{-\frac{|r_0\boldsymbol{\eta}|^2}{4}} e^{\frac{k_0^2}{4}\int_0^{2L} D(\boldsymbol{y}+\frac{\boldsymbol{\eta}\zeta}{k_0})-D(\boldsymbol{0})d\zeta} d\boldsymbol{\eta},\end{aligned}$$

where we used that $L/(k_0 r_0^2) \ll 1$. Substituting into (A3) gives (43).

Appendix B. Wigner Asymptotics

We cast the Wigner distribution in a suitable dimensionless form and present an asymptotic approximation valid in regime given by the scaling relation in Assumption (c). We state the result here for completeness, see [6] for a more complete discussion.

We consider the following Fourier transform V^{R} of the Wigner distribution W_k^{R}:

$$W_k^{\mathrm{R}}(z,\boldsymbol{x},\boldsymbol{x}',\boldsymbol{\kappa},\boldsymbol{\kappa}') = \frac{1}{(2\pi)^d}\int V_k^{\mathrm{R}}\Big(z,\frac{\boldsymbol{\kappa}+\boldsymbol{\kappa}'}{2},\boldsymbol{\kappa}-\boldsymbol{\kappa}',\boldsymbol{\kappa}''\Big) e^{i\boldsymbol{\kappa}''\cdot(\boldsymbol{x}'-\boldsymbol{x})} d\boldsymbol{\kappa}'', \quad \text{(B1)}$$

which we introduce because the stationary maps that we will identify in Lemma B.1, in the asymptotic regime $\alpha \to \infty$, have simple representations in this new frame. Note also that this ansatz incorporates the fact that W_k^{R} does not depend on $\boldsymbol{x}+\boldsymbol{x}'$, only on $\boldsymbol{x}-\boldsymbol{x}'$, $\boldsymbol{\kappa}$, and $\boldsymbol{\kappa}'$, which follows from the stationarity of the random medium. The Fourier-transformed operator $V_k^{\mathrm{R}}(z,\boldsymbol{\kappa},\boldsymbol{\kappa}',\boldsymbol{\kappa}'')$ has the form

$$V_k^{\mathrm{R}}(0,\boldsymbol{\kappa},\boldsymbol{\kappa}',\boldsymbol{\kappa}'') = \mathcal{R}_0^2(\pi l)^d e^{\frac{iz}{k}\boldsymbol{\kappa}'\cdot\boldsymbol{\kappa}''} \mathcal{V}^{\mathrm{R}}\Big(1,\boldsymbol{\kappa}l,\boldsymbol{\kappa}'l,\boldsymbol{\kappa}''l;\alpha(k,L),\beta(k,L)\Big), \quad \text{(B2)}$$

where $(\mathcal{V}^{\mathrm{R}}(\zeta,\boldsymbol{q},\boldsymbol{r},\boldsymbol{s};\alpha,\beta))_{\zeta\in[0,1]}$ is the solution of the dimensionless system

$$\begin{aligned}
\frac{\partial \mathcal{V}^{\mathrm{R}}}{\partial \zeta} = \frac{\beta}{(2\pi)^d}\int \hat{D}_0(\boldsymbol{u})\Big[&\mathcal{V}^{\mathrm{R}}\Big(\zeta,\boldsymbol{q}-\frac{1}{2}\boldsymbol{u},\boldsymbol{r}-\boldsymbol{u},\boldsymbol{s}\Big)e^{-i\alpha\boldsymbol{s}\cdot\boldsymbol{u}\zeta}\\
&+\mathcal{V}^{\mathrm{R}}\Big(\zeta,\boldsymbol{q}-\frac{1}{2}\boldsymbol{u},\boldsymbol{r}+\boldsymbol{u},\boldsymbol{s}\Big)e^{i\alpha\boldsymbol{s}\cdot\boldsymbol{u}\zeta}+\mathcal{V}^{\mathrm{R}}\Big(\zeta,\boldsymbol{q}-\frac{1}{2}\boldsymbol{u},\boldsymbol{r},\boldsymbol{s}-\boldsymbol{u}\Big)e^{-i\alpha\boldsymbol{r}\cdot\boldsymbol{u}\zeta}\\
&+\mathcal{V}^{\mathrm{R}}\Big(\zeta,\boldsymbol{q}-\frac{1}{2}\boldsymbol{u},\boldsymbol{r},\boldsymbol{s}+\boldsymbol{u}\Big)e^{i\alpha\boldsymbol{r}\cdot\boldsymbol{u}\zeta}-2\mathcal{V}^{\mathrm{R}}\big(\zeta,\boldsymbol{\kappa},\boldsymbol{r},\boldsymbol{s}\big)\\
&-\mathcal{V}^{\mathrm{R}}\Big(\zeta,\boldsymbol{q}-\frac{1}{2}\boldsymbol{u},\boldsymbol{r}-\boldsymbol{u},\boldsymbol{s}+\boldsymbol{u}\Big)e^{i\alpha[(\boldsymbol{r}-\boldsymbol{s})\cdot\boldsymbol{u}-|\boldsymbol{u}|^2]\zeta}\\
&-\mathcal{V}^{\mathrm{R}}\Big(\zeta,\boldsymbol{q}-\frac{1}{2}\boldsymbol{u},\boldsymbol{r}-\boldsymbol{u},\boldsymbol{s}-\boldsymbol{u}\Big)e^{-i\alpha[(\boldsymbol{r}+\boldsymbol{s})\cdot\boldsymbol{u}+|\boldsymbol{u}|^2]\zeta}\Big]d\boldsymbol{u}, \qquad \text{(B3)}
\end{aligned}$$

starting from $\mathcal{V}^{\mathrm{R}}(\zeta=0,\boldsymbol{q},\boldsymbol{r},\boldsymbol{s};\alpha,\beta)=\delta(\boldsymbol{q})$. Recall that $\alpha(k,L)=L/(kl^2)$ and $\beta(k,L)=\sigma^2k^2lL/4$.

The rapid transverse variations regime is particularly interesting to study because W_k^{R} has a multi-scale behavior. In (B3) this regime gives rise to rapid phases and this allows us to identify a simplified description and the multiscale behavior strongly influences the correlations. The following lemma describes the asymptotic behavior of $\mathcal{V}^{\mathrm{R}}$ as $\alpha\to\infty$. The presence of singular layers at $\boldsymbol{r}=\boldsymbol{0}$ and at $\boldsymbol{s}=\boldsymbol{0}$ requires particular attention and is responsible for instance for the enhanced backscattering phenomenon [6], (corresponding to part *(3)* in Lemma B.1). In general (part *(1)* in Lemma B.1) the Fourier-transformed operator decays exponentially according to the parameter $\beta D_0(\boldsymbol{0})$ corresponding to the total scattering cross section. This decay follows from a partial loss of coherence by random forward scattering. However, as articulated in parts *(2)* and *(3)* of the lemma below the coupling of wave modes depends on the full medium autocorrelation function if we look at nearby specular reflection and or small spatial offset frequencies. This coupling will be important in the analysis of the correlations in Section 7.2 and enhanced backscattering in Section 8. We have [6]

Lemma B.1:

(1) For any $\boldsymbol{r}\neq\boldsymbol{0}$, $\boldsymbol{s}\neq\boldsymbol{0}$:

$$\mathcal{V}^{\mathrm{R}}(\zeta,\boldsymbol{q},\boldsymbol{r},\boldsymbol{s};\alpha,\beta)\overset{\alpha\to\infty}{\longrightarrow}\delta(\boldsymbol{q})e^{-2\beta D_0(\boldsymbol{0})\zeta}. \qquad \text{(B4)}$$

(2) For any $\boldsymbol{s}\neq\boldsymbol{0}$ we have $\mathcal{V}^{\mathrm{R}}(\zeta,\boldsymbol{q},\frac{\boldsymbol{r}}{\alpha},\boldsymbol{s};\alpha,\beta)\overset{\alpha\to\infty}{\longrightarrow}\mathcal{V}^{\mathrm{R}}_{\boldsymbol{r}}(\zeta,\boldsymbol{q};\beta)$ where $\mathcal{V}^{\mathrm{R}}_{\boldsymbol{r}}(\zeta,\boldsymbol{q};\beta)$ is solution of

$$\frac{\partial \mathcal{V}^{\mathrm{R}}_{\boldsymbol{r}}}{\partial\zeta}=\frac{2\beta}{(2\pi)^d}\int\hat{D}_0(\boldsymbol{u})\left[\mathcal{V}^{\mathrm{R}}_{\boldsymbol{r}}\Big(\zeta,\boldsymbol{q}-\frac{1}{2}\boldsymbol{u}\Big)\cos\big(\boldsymbol{r}\cdot\boldsymbol{u}\zeta\big)-\mathcal{V}^{\mathrm{R}}_{\boldsymbol{r}}\big(\zeta,\boldsymbol{q}\big)\right]d\boldsymbol{u}, \qquad \text{(B5)}$$

and is given explicitly by

$$\mathcal{V}^{\mathrm{R}}_{\boldsymbol{r}}(\zeta,\boldsymbol{q};\beta)=\frac{1}{(2\pi)^d}\int e^{-i\boldsymbol{q}\cdot\boldsymbol{u}}e^{\beta\int_0^\zeta D_0(\frac{\boldsymbol{u}}{2}+\boldsymbol{r}\zeta')+D_0(\frac{\boldsymbol{u}}{2}-\boldsymbol{r}\zeta')-2D_0(\boldsymbol{0})d\zeta'}d\boldsymbol{u}. \qquad \text{(B6)}$$

Similarly, for any $\boldsymbol{r}\neq\boldsymbol{0}$ we have $\mathcal{V}^{\mathrm{R}}(\zeta,\boldsymbol{q},\boldsymbol{r},\frac{\boldsymbol{s}}{\alpha};\alpha,\beta)\overset{\alpha\to\infty}{\longrightarrow}\mathcal{V}^{\mathrm{R}}_{\boldsymbol{s}}(\zeta,\boldsymbol{q};\beta)$.

(3) For any $\boldsymbol{r}$ and $\boldsymbol{s}$ we have

$$\mathcal{V}^{\mathrm{R}}\Big(\zeta,\boldsymbol{q},\frac{\boldsymbol{r}}{\alpha},\frac{\boldsymbol{s}}{\alpha};\alpha,\beta\Big)\overset{\alpha\to\infty}{\longrightarrow}\mathcal{V}^{\mathrm{R}}_{\boldsymbol{r}}(\zeta,\boldsymbol{q};\beta)+\mathcal{V}^{\mathrm{R}}_{\boldsymbol{s}}(\zeta,\boldsymbol{q};\beta)-\delta(\boldsymbol{q})e^{-2\beta D_0(\boldsymbol{0})\zeta}. \quad \text{(B7)}$$

We next discuss the modification of the above result that follows from using a diffusive interface as introduced in Section 8.2. Under these conditions, the initial condition for the Wigner distribution is $W^R(z=L,\boldsymbol{x},\boldsymbol{x}',\boldsymbol{q},\boldsymbol{q}')=R_0^2\delta(\boldsymbol{x}-\boldsymbol{x}')\hat{\psi}(\boldsymbol{q}+\boldsymbol{q}')$. The associated initial condition for $\mathcal{V}^{\mathrm{R}}$ is $\mathcal{V}^{\mathrm{R}}(\zeta=0,\boldsymbol{q},\boldsymbol{r},\boldsymbol{s})=(\pi l)^{-d}\hat{\psi}(2\boldsymbol{q}/l)$. The Lemma B.1 is then modified as follows

Lemma B.2:

(1) For any $\boldsymbol{r}\neq\boldsymbol{0}$, $\boldsymbol{s}\neq\boldsymbol{0}$:

$$\mathcal{V}^{\mathrm{R}}(\zeta,\boldsymbol{q},\boldsymbol{r},\boldsymbol{s};\alpha,\beta)\overset{\alpha\to\infty}{\longrightarrow}(\pi l)^{-d}\hat{\psi}(2\boldsymbol{q}/l)e^{-2\beta D_0(\boldsymbol{0})\zeta}. \quad \text{(B8)}$$

(2) For any $\boldsymbol{s}\neq\boldsymbol{0}$ we have $\mathcal{V}^{\mathrm{R}}(\zeta,\boldsymbol{q},\frac{\boldsymbol{r}}{\alpha},\boldsymbol{s};\alpha,\beta)\overset{\alpha\to\infty}{\longrightarrow}\mathcal{V}^{\mathrm{R}}_{\boldsymbol{r}}(\zeta,\boldsymbol{q};\beta)$ where $\mathcal{V}^{\mathrm{R}}_{\boldsymbol{r}}(\zeta,\boldsymbol{q};\beta)$ is solution of

$$\frac{\partial\mathcal{V}^{\mathrm{R}}_{\boldsymbol{r}}}{\partial\zeta}=\frac{2\beta}{(2\pi)^d}\int\hat{D}_0(\boldsymbol{u})\left[\mathcal{V}^{\mathrm{R}}_{\boldsymbol{r}}\Big(\zeta,\boldsymbol{q}-\frac{1}{2}\boldsymbol{u}\Big)\cos\big(\boldsymbol{r}\cdot\boldsymbol{u}\zeta\big)-\mathcal{V}^{\mathrm{R}}_{\boldsymbol{r}}\big(\zeta,\boldsymbol{q}\big)\right]d\boldsymbol{u}, \quad \text{(B9)}$$

and is given explicitly by

$$\mathcal{V}^{\mathrm{R}}_{\boldsymbol{r}}(\zeta,\boldsymbol{q};\beta)=\frac{1}{(2\pi)^d}\int\psi\left(\frac{l\boldsymbol{u}}{2}\right)e^{-i\boldsymbol{q}\cdot\boldsymbol{u}}e^{\beta\int_0^\zeta D_0(\frac{\boldsymbol{u}}{2}+\boldsymbol{r}\zeta')+D_0(\frac{\boldsymbol{u}}{2}-\boldsymbol{r}\zeta')-2D_0(\boldsymbol{0})d\zeta'}d\boldsymbol{u}. \quad \text{(B10)}$$

Similarly, for any $\boldsymbol{r}\neq\boldsymbol{0}$ we have $\mathcal{V}^{\mathrm{R}}(\zeta,\boldsymbol{q},\boldsymbol{r},\frac{\boldsymbol{s}}{\alpha};\alpha,\beta)\overset{\alpha\to\infty}{\longrightarrow}\mathcal{V}^{\mathrm{R}}_{\boldsymbol{s}}(\zeta,\boldsymbol{q};\beta)$.

(3) For any $\boldsymbol{r}$ and $\boldsymbol{s}$ we have

$$\mathcal{V}^{\mathrm{R}}\Big(\zeta,\boldsymbol{q},\frac{\boldsymbol{r}}{\alpha},\frac{\boldsymbol{s}}{\alpha};\alpha,\beta\Big)\overset{\alpha\to\infty}{\longrightarrow}\mathcal{V}^{\mathrm{R}}_{\boldsymbol{r}}(\zeta,\boldsymbol{q};\beta)+\mathcal{V}^{\mathrm{R}}_{\boldsymbol{s}}(\zeta,\boldsymbol{q};\beta)-(\pi l)^{-d}\hat{\psi}(2\boldsymbol{q}/l)e^{-2\beta D_0(\boldsymbol{0})\zeta}. \quad \text{(B11)}$$

Proof. In case *(1)*, the rapid phases cancel the contributions of all but the term $\mathcal{V}^R(\zeta,\boldsymbol{q},\boldsymbol{r},\boldsymbol{s})$ in (B3), and we get

$$\frac{\partial\mathcal{V}^R}{\partial\zeta}=-2\frac{\beta}{(2\pi)^d}\int\hat{\mathcal{C}}_0(\boldsymbol{u})\mathcal{V}^R d\boldsymbol{u}=-2\beta\mathcal{C}_0(\boldsymbol{0})\mathcal{V}^R,$$

which gives (B4) and (B8) in view of the corresponding initial conditions. In case *(2)*, we obtain in the limit $\alpha\to\infty$ the simplified system

$$\frac{\partial\tilde{\mathcal{V}}^R_{\boldsymbol{r}}}{\partial\zeta}=\frac{\beta}{(2\pi)^d}\int\hat{\mathcal{C}}_0(\boldsymbol{u})\Big[\tilde{\mathcal{V}}^R_{\boldsymbol{r}}\Big(\zeta,\boldsymbol{q}-\frac{1}{2}\boldsymbol{u},\boldsymbol{s}-\boldsymbol{u}\Big)e^{-i\boldsymbol{r}\cdot\boldsymbol{u}\zeta}$$
$$+\tilde{\mathcal{V}}^R_{\boldsymbol{r}}\Big(\zeta,\boldsymbol{q}-\frac{1}{2}\boldsymbol{u},\boldsymbol{s}+\boldsymbol{u}\Big)e^{i\boldsymbol{r}\cdot\boldsymbol{u}\zeta}-2\tilde{\mathcal{V}}^R_{\boldsymbol{r}}\big(\zeta,\boldsymbol{q},\boldsymbol{s}\big)\Big]d\boldsymbol{u}.$$

We then Fourier transform this equation in $\boldsymbol{q}$ and $\boldsymbol{s}$, and we obtain that the solution does not depend on $\boldsymbol{s}$, that it satisfies (B5), and that it is given by (B6) and (B10).

In case *(3)* we obtain the simplified system for $\mathcal{V}^R_{\boldsymbol{r},\boldsymbol{s}}(\zeta,\boldsymbol{q})$ =

$\lim_{\alpha\to\infty}\mathcal{V}^R\big(\zeta,\boldsymbol{q},\frac{\boldsymbol{r}}{\alpha},\frac{\boldsymbol{s}}{\alpha}\big)$:

$$\frac{\partial \mathcal{V}^R_{\boldsymbol{r},\boldsymbol{s}}}{\partial\zeta} = \frac{2\beta}{(2\pi)^d}\int \hat{\mathcal{C}}_0(\boldsymbol{u})\Big[\mathcal{V}^R_{\boldsymbol{s}}\Big(\zeta,\boldsymbol{q}-\frac{1}{2}\boldsymbol{u}\Big)\cos\big(\boldsymbol{s}\cdot\boldsymbol{u}\zeta\big) + \mathcal{V}^R_{\boldsymbol{r}}\Big(\zeta,\boldsymbol{q}-\frac{1}{2}\boldsymbol{u}\Big)\cos\big(\boldsymbol{r}\cdot\boldsymbol{u}\zeta\big) - \mathcal{V}^R_{\boldsymbol{r},\boldsymbol{s}}\big(\zeta,\boldsymbol{q}\big)\Big]d\boldsymbol{u}.$$

Using the equation (B5) satisfied by $\mathcal{V}^R_{\boldsymbol{s}}$ and $\mathcal{V}^R_{\boldsymbol{r}}$, we get

$$\frac{\partial \mathcal{V}^R_{\boldsymbol{r},\boldsymbol{s}}}{\partial\zeta} = \frac{\partial \mathcal{V}^R_{\boldsymbol{r}}}{\partial\zeta} + \frac{\partial \mathcal{V}^R_{\boldsymbol{s}}}{\partial\zeta} + 2\beta\mathcal{C}_0(\boldsymbol{0})\left[\mathcal{V}^R_{\boldsymbol{r}} + \mathcal{V}^R_{\boldsymbol{s}} - \mathcal{V}^R_{\boldsymbol{r},\boldsymbol{s}}\right],$$

which yields (B7) and (B11). □

Appendix C. Enhanced Backscattered Intensity

We derive the result (49). Using (48) we first find

$$\lim_{\varepsilon\to 0}\mathrm{E}\left[\left|\widetilde{v}^\varepsilon_1(s,\boldsymbol{\kappa}_0)\right|^2\right] = \mathcal{R}_0^2|f_0^\delta(s)|^2 I^R(\boldsymbol{\kappa}_0),$$

for

$$I^R(\boldsymbol{\kappa}_0) = \frac{1}{\mathcal{R}_0^2}\iint \mathrm{E}\Big[\widehat{\boldsymbol{\mathcal{R}}}^\varepsilon(k_0,0,\boldsymbol{\kappa}_0-k_0\boldsymbol{\theta},\boldsymbol{\kappa}_1'+k_0\boldsymbol{\theta}) \times\overline{\widehat{\boldsymbol{\mathcal{R}}}^\varepsilon(k_0,0,\boldsymbol{\kappa}_0-k_0\boldsymbol{\theta},\boldsymbol{\kappa}_2'+k_0\boldsymbol{\theta})}\Big]\hat{g}_{\rm inc}(\boldsymbol{\kappa}_1')\overline{\hat{g}_{\rm inc}(\boldsymbol{\kappa}_2')}d\boldsymbol{\kappa}_1'd\boldsymbol{\kappa}_2'.$$

In view of (28) and (A1) we have

$$\begin{aligned}
\mathrm{E}\left[\widehat{\boldsymbol{\mathcal{R}}}^\varepsilon(k_0,0,\boldsymbol{\kappa}_0,\boldsymbol{\kappa}_1')\overline{\widehat{\boldsymbol{\mathcal{R}}}^\varepsilon(k_0,0,\boldsymbol{\kappa}_0,\boldsymbol{\kappa}_2')}\right] &= \frac{1}{(2\pi)^{4d}}\iint e^{-i(\boldsymbol{x}\cdot\boldsymbol{\kappa}_0-\boldsymbol{x}'\cdot\boldsymbol{\kappa}_1')}e^{i(\tilde{\boldsymbol{x}}\cdot\boldsymbol{\kappa}_0-\tilde{\boldsymbol{x}}'\cdot\boldsymbol{\kappa}_2')}\\
&\quad\times e^{i\boldsymbol{q}\cdot(\boldsymbol{x}-\tilde{\boldsymbol{x}})}e^{i\boldsymbol{q}'\cdot(\boldsymbol{x}'-\tilde{\boldsymbol{x}}')}W^R_{k_0}(0,(\boldsymbol{x}+\tilde{\boldsymbol{x}})/2,(\boldsymbol{x}'+\tilde{\boldsymbol{x}}')/2,\boldsymbol{q},\boldsymbol{q}')d\boldsymbol{x}d\boldsymbol{x}'d\tilde{\boldsymbol{x}}d\tilde{\boldsymbol{x}}'d\boldsymbol{q}d\boldsymbol{q}'\\
&= \frac{1}{(2\pi)^{4d}}\iint e^{-i\boldsymbol{\kappa}_0\cdot\boldsymbol{z}}e^{i(\tilde{\boldsymbol{z}}'+\boldsymbol{z}'/2)\cdot\boldsymbol{\kappa}_1'}e^{-i(\tilde{\boldsymbol{z}}'-\boldsymbol{z}'/2)\cdot\boldsymbol{\kappa}_2'}\\
&\quad\times e^{i\boldsymbol{q}\cdot\boldsymbol{z}}e^{i\boldsymbol{q}'\cdot\boldsymbol{z}'}W^R_{k_0}(0,\tilde{\boldsymbol{z}},\tilde{\boldsymbol{z}}',\boldsymbol{q},\boldsymbol{q}')d\boldsymbol{z}d\boldsymbol{z}'d\tilde{\boldsymbol{z}}d\tilde{\boldsymbol{z}}'d\boldsymbol{q}d\boldsymbol{q}'\\
&= \frac{1}{(2\pi)^{2d}}\iint e^{i\tilde{\boldsymbol{z}}'\cdot(\boldsymbol{\kappa}_1'-\boldsymbol{\kappa}_2')}\delta(\boldsymbol{q}-\boldsymbol{\kappa}_0)\delta(\boldsymbol{q}'+\boldsymbol{\kappa}_1'/2+\boldsymbol{\kappa}_2'/2)\\
&\quad\times W^R_{k_0}(0,\tilde{\boldsymbol{z}},\tilde{\boldsymbol{z}}',\boldsymbol{q},\boldsymbol{q}')d\tilde{\boldsymbol{z}}d\tilde{\boldsymbol{z}}'d\boldsymbol{q}d\boldsymbol{q}'.
\end{aligned}$$

This gives

$$I^R(\boldsymbol{\kappa}_0) = \frac{1}{(2\pi)^{2d}\mathcal{R}_0^2}\iint W^R_{k_0}(0,\tilde{\boldsymbol{z}},\tilde{\boldsymbol{z}}',\boldsymbol{\kappa}_0-k_0\boldsymbol{\theta},-(\boldsymbol{\kappa}_1'+\boldsymbol{\kappa}_2')/2-k_0\boldsymbol{\theta}) \times e^{i\tilde{\boldsymbol{z}}'\cdot(\boldsymbol{\kappa}_1'-\boldsymbol{\kappa}_2')}\hat{g}_{\rm inc}(\boldsymbol{\kappa}_1')\overline{\hat{g}_{\rm inc}(\boldsymbol{\kappa}_2')}d\tilde{\boldsymbol{z}}d\tilde{\boldsymbol{z}}'d\boldsymbol{\kappa}_1'd\boldsymbol{\kappa}_2'.$$

In view of (B1) we have

$$\iint W^R_{k_0}(0, \tilde{\boldsymbol{z}}, \tilde{\boldsymbol{z}}', \boldsymbol{\kappa}_0, -(\boldsymbol{\kappa}'_1 + \boldsymbol{\kappa}'_2)/2) e^{i\tilde{\boldsymbol{z}}'\cdot(\boldsymbol{\kappa}'_1 - \boldsymbol{\kappa}'_2)} d\tilde{\boldsymbol{z}} d\tilde{\boldsymbol{z}}'$$
$$= (2\pi)^d V^R(0, (\boldsymbol{\kappa}_0 - \boldsymbol{\kappa}'_1)/2, \boldsymbol{\kappa}_0 + \boldsymbol{\kappa}'_1, \boldsymbol{0}) \delta(\boldsymbol{\kappa}'_1 - \boldsymbol{\kappa}'_2).$$

Then, using (B2) we find

$$I^R(\boldsymbol{\kappa}_0) = (l/2)^d \int \mathcal{V}^R(1, l(\boldsymbol{\kappa}_0 - \boldsymbol{\kappa}' - 2k_0\boldsymbol{\theta})/2, l(\boldsymbol{\kappa}_0 + \boldsymbol{\kappa}'), \boldsymbol{0}; \alpha(k_0, L), \beta(k_0, L))$$
$$\times |\hat{g}_{\rm inc}(\boldsymbol{\kappa}')|^2 d\boldsymbol{\kappa}'.$$

References

[1] A. Bamberger, B. Engquist, L. Halpern, and P. Joly, Parabolic wave equation approximations in heterogeneous media, SIAM J. Appl. Math. **48** (1988), 99-128.

[2] Y. N. Barabanenkov, Wave corrections for the transfer equation for backward scattering, Izv. Vyssh. Uchebn. Zaved. Radiofiz. **16** (1973), 88–96.

[3] C. Bernardi and M.-C. Pelissier, Spectral approximation of a Schrödinger type equation, Mathematical Models and Methods in Applied Sciences **4** (1994), 49–88.

[4] D. Dawson and G. Papanicolaou, A random wave process, Appl. Math. Optim. **12** (1984), 97–114.

[5] J. Garnier and K. Sølna, Random backscattering in the parabolic scaling, *J. Stat. Phys.* **131** (2008), 445–486.

[6] J. Garnier and K. Sølna, Coupled paraxial wave equations in random media in the white-noise regime, Ann. Appl. Probab. **19** (2009), 318–346.

[7] Z. H. Gu, J. Lu, and A. A. Maradudin, Enhanced backscattering from a rough dielectric film on a glass substrate, J. Opt. Soc. Am. A. **10** (1993), 1753–1764.

[8] G. Labeyrie, F. de Tomasi, J.-C. Bernard, C. A. Müller, C. Miniatura, and R. Kaiser, Coherent backscattering of light by atoms, Phys. Rev. Lett. **83** (1999), 5266–5269.

[9] M. C. W. van Rossum and Th. M. Nieuwenhuizen, Multiple scattering of classical waves: microscopy, mesoscopy, and diffusion, Rev. Mod. Phys. **71** (1999), 313–371.

[10] A. Tourin, A. Derode, P. Roux, B. A. van Tiggelen, and M. Fink, Time-dependent coherent backscattering of acoustic waves, Phys. Rev. Lett. **79** (1997), 3637–3639.

[11] M. P. van Albada and A. Lagendijk, Observation of weak localization of light in a random medium, Phys. Rev. Lett. **55** (1985), 2692–2695.

[12] P. E. Wolf and G. Maret, Weak localization and coherent backscattering of photons in disordered media, Phys. Rev. Lett. **55** (1985), 2696–2699.